UNIVERSITÀ DI PISA

Facoltà di Ingegneria

Laurea Specialistica in Ingegneria dell'Automazione

A NEW APPROACH TO MODELING MORPHOGENESIS USING CONTROL THEORY

Candidato:

Giulio Telleschi

Tesi di laurea

Relatori:

Prof. Andrea Caiti - Università di Pisa

Prof. Monique Chyba - University of Hawaii

Sessione di Laurea del 11/05/2012
Archivio tesi Laurea Specialistica in Ingegneria dell'Automazione
Anno accademico 2011/2012

ACKNOWLEDGMENTS

First and foremost, I would like to thank Professor Andrea Caiti for the great opportunity he offered me and for his constant enthusiasm supporting my work, and Dr. Monique Chyba for letting me join her research group, motivating me as no one else did before and have a unique chance to grow professionally. Without them, this thesis would not have been possible.

I would also like to thank John Rader for his guidance and for the fair team work we made together, and Aaron Tamura Sato for his technical support. Finally, I would like to thank the Departments of Mathematics and of Mechanical Engineering at the University of Hawaii, in the person of Dr. M. Kobayashi, for treating me as a peer and giving me a lot of gratification.

Ringrazio la mia famiglia, in ogni sua colorata declinazione, per il supporto incessante in tutti gli anni di studi e per il costante incoraggiamento che mi ha fornito anche nei momenti più difficili; Azzurra per avermi accompagnato in un'altra importantissima tratta di questo straordinario percorso e tutti gli amici, *even the Hawaiian ones of course*, senza i quali non sarei potuto essere ciò che sono.

A chi non c'è più,

perché ci sarà sempre.

ABSTRACT

It has been proposed that biological structures termed fractones may govern morphogenic events of cells; that is, fractones may dictate when a cell undergoes mitosis by capturing and concentrating certain chemical growth factors created by cells in their immediate vicinity. Based on this hypothesis, we present a model of cellular growth that incorporates these fractones, freely-diffusing growth factor, their interaction with each other, and their effect on cellular mitosis. The question of how complex biological cell structures arise from single cells during development can now be posed in terms of a mathematical control problem in which the activation and deactivation of fractones determines how a cellular mass forms. Stated in this fashion, several new questions in the field of control theory emerge as the configuration space is constantly evolving (caused by the creation of new cells), and thus cannot be analyzed using traditional techniques of control theory. We present this new class of problems, as well as an initial analysis of some of these questions. Also, we indicate an extension of the proposed control method to layout optimization.

SOMMARIO

Recenti studi hanno evidenziato l'esistenza di strutture biologiche, chiamate *frattoni*, in grado di controllare la morfogenesi delle cellule. I *frattoni* quindi, assorbendo i fattori di crescita prodotti dalle cellule nelle loro immediate vicinanze, danno l'input affinché le cellule procedano alla mitosi. In base a queste ipotesi, proponiamo un modello di crescita cellulare che include i *frattoni*, i fattori di crescita liberi di diffondersi nello spazio, le interazioni che ne scaturiscono e il conseguente effetto sulla duplicazione cellulare. Possiamo dunque formulare in termini matematici e di controllo il problema della formazione di una struttura biologica complessa composta dalle cellule per la quale l'attivazione e la disattivazione dei *frattoni* determina lo sviluppo della struttura. Definendo il problema in questi termini, sorgono molte domande nel campo della teoria del controllo poiché lo spazio di operativo è in continua evoluzione (a causa della creazione di nuove cellule) e quindi non può essere condotta un'analisi mediante le tradizionali tecniche della teoria del controllo. Attraverso questo studio, presentiamo una nuova classe di problemi unitamente ad una prima analisi delle domande che ne scaturiscono. Infine, è mostrata una possibile estensione del modello all'ottimizzazione di layout.

LIST OF CONTENTS

LIST OF FIGURES

LIST OF TABLES

INTRODUCTION

All vertebrate animals, including humans, produce new neurons and glia (the two primary specialized cell types of the brain) throughout life. Neurons and glia derive from neural stem cells, which reside, proliferate, and differentiate in specialized zones termed niches. Neural stem cells proliferate extensively during development and progressively generate the brain, a phenomenon named neurulation, or brain morphogenesis. Interestingly, neural stem cells exist and continue to generate neurons and glial cells after birth and throughout adulthood in very restricted niches, primarily the walls of the lateral ventricle. What are the mechanisms that control neural stem cell proliferation and differentiation? Neural stem cells and their progeny respond to growth factors, endogenous signaling molecules that circulate in the extracellular milieu (in between cells).

The process of neurulation and subsequent events of the brain's formation involve multiple growth factors that induce proliferation, differentiation, and migration of cells. The distribution and activation of these growth factors in space and time will determine the morphogenic events of the developing mamalian brain. However, the process organizing the distribution and availability of growth factors within the neuroepithelium is not understood. Structures, termed fractones, directly contact neural stem and progenitor cells, capture and concentrate said growth factors, and are associated with cell proliferation ([1], [2], [3]). Hence, our hypothesis is that fractones are the captors that spatially control the activation of growth factors in a precise location to generate a morphogenic event.

Inspired by these biological discoveries, we propose to develop and analyze a mathematical model predicting cell proliferation from the spatial distribution of fractones. Dynamic mathematical modeling, i.e. models that represent change in rates over time, serves several purposes [4]. Using computer simulations, by mimicking the assumed forces resulting in a system behavior, the model helps us to understand the nonlinear dynamics of the system under study. Such approach is especially well suited

for biological systems whose complexity renders a purely analytical approach unrealistic. Moreover, it allows us to overcome the excessively demanding purely experimental approach to understand a biological system. Our primary goal in this paper is to develop a model that contains the crucial features of our hypothesis and, at the same time, is sufficiently simple to allow an understanding of the underlying principles of the observed system.

We propose to model this biological process as a control system, the control depicting the spatial distribution of the active fractones. This is a novel approach with respect to the most commonly reaction-diffusion models seen in the literature on morphogenesis, however it is not that surprising. Indeed, control theory is instrumental to overcome many challenges faced by scientists to design systems with a very high degree of complexity and interaction with the environment ([5], [6], [7]). Examples of its applicability in physical and biological systems are numerous ([8], [9]).

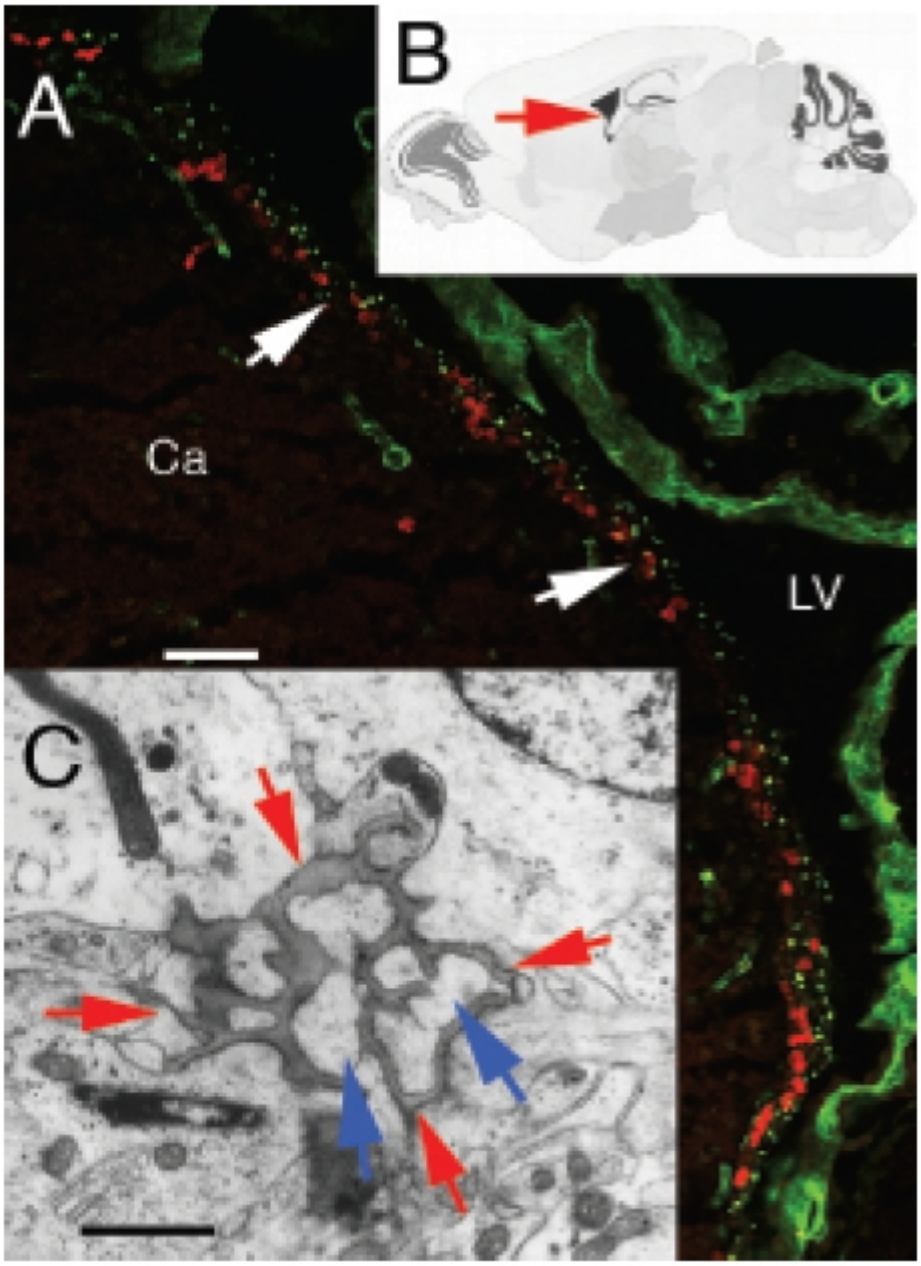

Figure 1 - Fractones are extracellular matrix structures associated with proliferating cells in the neurogenic zone (neural stem cell niche) of the adult mammalian brain.[1]

[1] (A) Visualization of fractones (green, puncta, arrows) by confocal laser scanning microscopy in the primary neurogenic zone of the adult mouse brain, i.e. the wall of the lateral ventricle (LV) at the surface of the caudate nucleus (Ca). Each green puncta is an individual fractone. The red puncta indicate proliferating neural stem cells and progenitor cells immunolabeled for the mitotic marker bromodeoxyuridine. Stem cells and their progeny proliferate next to fractones (arrows). (B) Location of the confocal image A (arrow) in a schematic representation of the mouse brain (cut in the sagittal plane). (C) Visualization of an individual fractone by transmission electron microscopy (dark-grey structure indicated by the four red arrows. The processes of neural stem cells and of their progeny, which appear light-grey (blue arrows) are inserted into the folds of the fractone. Scale bars. A: 50 μm; C: 1 μm.

Historical Usage of Mathematics in Biology

The history of mathematics used to solve problems arising from biology dates back several hundred years to the times of Bernoulli and Euler. Prior to the mid-1900s, though, biology served primarily as the inspiration to understanding larger problems rather than as a practical field to be studied under the rigors of applied mathematics. Many problems in the field, even simplified with strong assumptions and in their least-complex forms, were unable to be solved using traditional techniques of mathematicians due to their complexity. Researchers of the day were either forced to pay understudies to perform hundreds, perhaps thousands, of hand calculations, or they would make drastic simplifications of their models merely to gain insight into the behavior of the system, and, as a consequence, many would make incorrect conclusions when compared versus real-world data. However, at times, some models were found to be accurate when compared to known data, and thus were accepted as theory (this is most likely due to acceptable simplifications, those not significant to the model as a whole).

Once the mid-20th century arrived, and with it the advent of the computer, researchers finally had the luxury of being able to analyze complex systems without unnecessary simplifications. And with the creation of the personal computer and modern computational software (as well as the internet and supercomputing clusters) in the 1980s, scientists and researchers could now fully model the most complex system without any necessary simplifications and can find solutions (albeit numeric) for a variety of problems.

Much of what has been attempted to solve or has been solved using mathematics in the field of biology is summarized in Table 1.

Historical Usage of Control Theory in Biology

The appearance and usage of control theory in the field of biology is a relatively new idea, dating back only a few decades. The first real evidence of the usage of control theory to understand a biological process originates with Norbert Wiener [10], who developed many of the ideas of feedback and filtering in the early 1940s in collaboration with the Harvard physiologist Arturo Rosenblueth, who was, in turn, heavily influenced by the work of his colleague Walter Cannon [11], who coined the

term homeostasis in 1932 to refer to feedback mechanisms for set-point regulation in living organisms. Rudolf Kalman [12] often used biological analogies in his discussion of control systems theory, and so did many other early researchers. Modern biological control, enveloped in the more general field of systems biology, emanates from the work of Ludwig von Bertalanffy [13] with his general systems theory. One of the first numerical simulations in biology was published in 1952 by the British neurophysiologists and Nobel prize winners Alan Hodgkin and Andrew Huxley [14], who constructed a mathematical model that explained the action potential propagating along the axon of a neuronal cell. Also, in 1960, Denis Noble [15], using computer models of biological organs and organ systems to interpret function from the molecular level to the whole organism, developed the first computer model of the heart pacemaker. The formal study of systems biology, as a distinct discipline, was launched by systems theorist Mihajlo Mesarovic in 1966 with an international symposium at the Case Institute of Technology in Cleveland, Ohio entitled "Systems Theory and Biology" [16].

Subject	**Reference**
Spread of diseases	Bernoulli 1760 [17]
Fluid mechanics of blood flow	Euler 1760 [18]
Age structure of stable populations	Euler 1775 [19]
Logistic equation for limited population growth	Verhulst 1838 [20]
Branching processes, extinction of family names	Galton 1889 [21]
Correlation	Pearson 1903 [22]
Markov chains, statistics of language	Markov 1906 [23]
Hardy-Weinberg equilibrium in population genetics	Hardy 1908 [24]
Dynamics of interacting species	Lotka 1925 [25]; Volterra 1931 [26]

Traveling waves in genetics	Kolmogorov 1937 [27]
Distribution for estimating bacterial mutation rates	Luria 1943 [28]
Birth process, birth and death process	Kendall 1949 [29]
Morphogenesis	Turing 1952 [30]
Game theory	Von Neumann 1953 [31]
Circular interval graphs, genetic fine structure	Benzer 1959 [32]
Threshold functions of random graphs	Erdös 1960 [33]
Sampling formula for haplotype frequencies	Ewens 1972 [34]
Coalescent genealogy of populations	Kingman 1982 [35]
Diffusion equation for gene frequencies	Kimura 1994 [36]

Table 1 - Mathematics Arising from Biological Problems

The field of systems biology is large and encompassing, so much so that it, at times, is hard to define what is and is not part of the field. However, the kinds of research and problems that have laid the groundwork for establishing the field are as follows:

- complex molecular systems, such as the metabolic control analysis and the biochemical systems theory between 1960-1980 ([37] , [38])
- quantitative modeling of enzyme kinetics, a discipline that flourished, between 1900 and 1970 [39]
- mathematical modeling of population growth
- simulations developed to study neurophysiology
- control theory and cybernetics [40]

Some recent problems approached by those studying control theory in the field of biology have been to model, among others:

- internal workings of the cell
- molecular signaling or energy transfer (among RNA, DNA, proteins, etc.)

- cell signal transduction processes
- neural pathways
- regulation versus homeostasis
- RNA/DNA transcription with an emphasis on mutation
- gene function and interactions.

The breadth and variety of problems that can be modeled using control theory runs the gamut, from the molecular through the microscopic up to the macroscopic. Many areas of biology have been affected by many areas of mathematical science, and the challenges of biology have also prompted advances of importance to the mathematical sciences themselves. The rapidly developing field of systems biology (the merging of biology, physics, engineering, and/or mathematics) is tremendously exciting, and full of unique research opportunities and challenges, especially for the application of control theory.

Motivation

This research has been held towards three different fields of science: biology, mathematics and engineering.

Biological Motivation

A fundamental problem is to understand how growth factors control the topology of cell proliferation and direct the construction of the forming neural tissue. It has been demonstrated that extra-cellular matrix (ECM) molecules strongly influence growth factor-mediated cell proliferation. ECM proteoglycans can capture and present growth factors to the cell surface receptors to ultimately trigger the biological response of growth factors. Hence, by building a model that incorporates the most important features of the biological system, we attempt to simulate how this occurs to give more insight into how structure of biological systems takes shape under the assumption that it is driven by the presence of growth factors and activation by ECM molecules, particularly fractones.

F.Mercier and his collaborators have discovered ECM structures that are associated with proliferating cells in the stem cell niche of the adult mammalian brain ([1], [2], [3]). These structures, termed fractones, hold a high potential as captors of mitotic and neurogenic growth factors. In Figure 2 (*A*) we have a laser scanning confocal microscopy image showing the section of the whole head of an E9.5 embryo (9.5 days post-coitum). Proliferating neuroepithelial cells were visualized by phosphorylated histone-3 (PH3, a marker of mitosis) immunofluorescence cytochemistry (red). The extracellular matrix material was revealed by immunoreactivity for laminin, a ubiquitous glycoprotein found in basement membranes and fractones. However, fractones are too small to be visualized at this level of magnification. Note that cells proliferate near the lumen of the forming cavity (arrow, neural groove). The plan of section is indicated in the inset. (*B*) High magnification confocal microscopy field showing proliferating neuroepithelial cells (PH3 immunoreactivity, red) associated with fractone (green punctae) at E8.5. (*C*) Magnification of the area indicated by an arrow in A showing that neuroepithelial cells also proliferate (red) next to fractones (green punctae, arrow) at E9.5.

During our research, we analyzed a space in which there exist three unique components: fractones, cells/holes, and growth factors (GFs) that cells produce. The initial configuration is (at least) one cell and one associated fractone. The cells produce growth factors on a fixed, regular time interval and in discrete amounts. The time at which an individual cell produces growth factor, however, may be different from any other cell (depending on when each cell entered the system). Once produced, the GFs diffuse radially away from the cell into the extra-cellular diffusion space that occurs between cells. The GFs do not chemically interact with each other, and they are actively trapped by a fractone when significantly close. Once a fractone has absorbed enough GF beyond some threshold, it sends a signal to the associated cell(s) to undergo mitosis. A hole is similar to a cell, except that it does not produce GF. In fact, a hole can be thought of as a wall, a non-interacting object that the system evolves around.

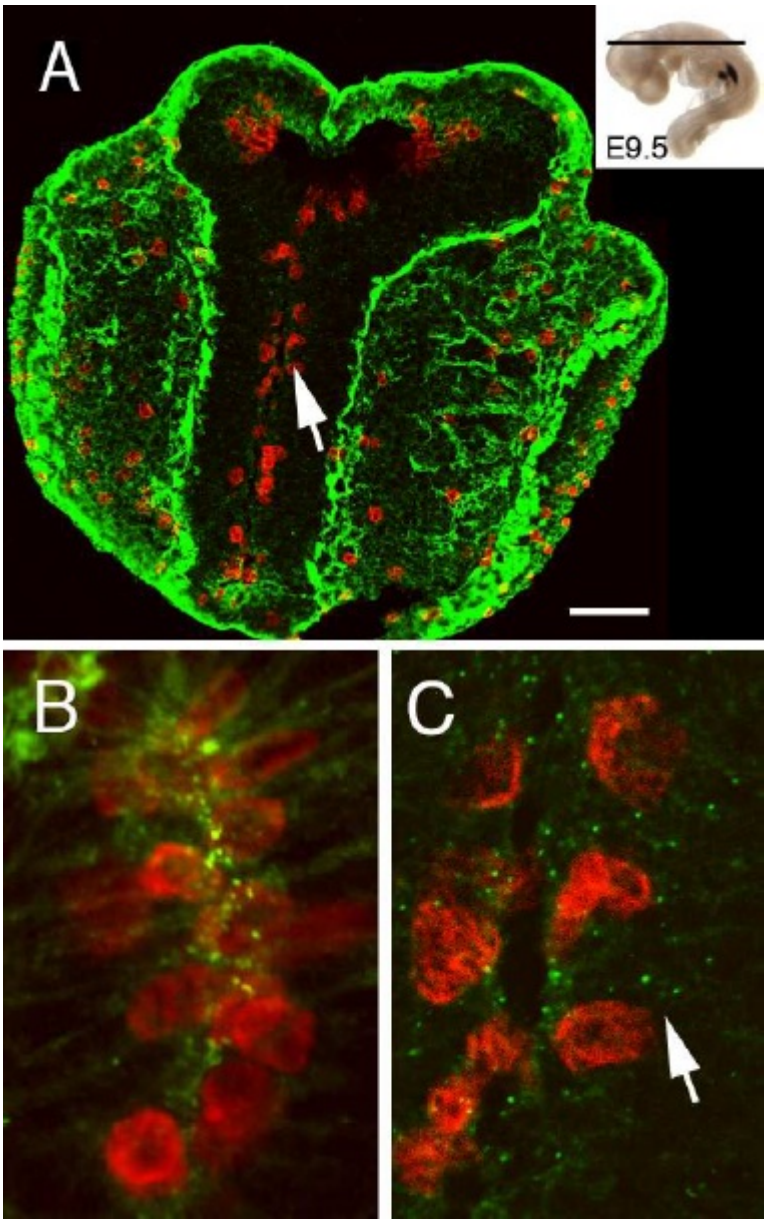

Figure 2 - Characterization of fractones in the mouse neuroepithelium during brain morphogenesis

Mathematical Motivation

The classical models attempting to describe morphogenesis are based on Reaction-Diffusion (RD) equations developed in Turing's "Morphogenesis" [30]. Although Turing made a great attempt to mathematically portray morphogenesis, his work is not an adequate model to describe the system given new discoveries and developments since the 1950s. With his model, Turing was describing how reactive chemicals present

in a static, living structure interact in a continuous medium (a skin tissue, for example) via diffusion (and, surprisingly, form wave-like patterns). For the system we are describing, reaction-diffusion equations cannot be used to study the mechanisms of morphogenesis during development as the growth factors are non-interacting.

Turing's hypothesis came from the simplistic approach that diffusion and subsequent chemical reactions of an activator/inhibitor pair of chemicals are what drive pattern formation, leading to the following equations for a one dimensional model:

$$\dot{X}_r = f\left(X_r\right) + \mu\left(X_{r+1} - 2X_r + X_{r-1}\right), \quad for\ r = 1, \ldots, N$$

where N represents the number of cells in the system, X is the concentration of morphogens and μ is a diffusion constant.

Since growth factors are non-reactive, we should not use the reaction function $f\left(X_r\right)$.

To expand this model to higher dimensions, the equation must accommodate more neighbors. Thus, the 2D diffusion equation is:

$$\dot{X}_{(i,j)} = f\left(X_{(i,j)}\right) + \mu\left(X_{(i+1,j)} + X_{(i-1,j)} + X_{(i,j+1)} + X_{(i,j-1)} - 4X_{(i,j)}\right)$$

Based on the hypothesis of ([1], [2], [3]), morphogenesis involves the capture and activation of growth factors by fractones at specific locations according to a precise timing. Also, Turing's assumption of unchanging state space (i.e. there is no growth, or the cells do not replicate) is not applicable to our model since, as cells replicate, the system of equations describing the "diffusion-trapping" model grows by one equation for every new cell produced. This adds mathematical complexity to the problem in that the system of equations governing the model are increasing in number. As mentioned before, the fractones influence GF-mediated cell proliferation, which is also a sign that Turing's model will not suffice, as there is no mechanism in the reaction-diffusion equations for structures with this type of action. Moreover, the distribution of fractones is constantly changing during development, reflecting the dynamics of the morphogenic events. Therefore, the organizing role of fractones in morphogenesis must be analyzed by an alternative mathematical model.

Engineering Motivation

As part of engineering design, layout optimization plays a critical role in the pursuit of optimal design. Layout optimization aims at finding the optimum distribution or layout of material within a bounded domain, called the design domain, that minimizes an objective or target function, while satisfying a set of constraints (see the recent monograph and reviews ([41], [42] , [43])).

Existing topology optimization methods rest on mathematical foundations (see, for example, [41], [44]). And mathematically, the search space, where the optimization layout is defined, is a topological vector space of infinite dimension - usually a Sobolev space [44]. In practice, however, computational methods used to solve layout optimization can only store and compute finite amount of data. This limitation forces any numerical optimization methods to rely on approximations of the search space and of the admissible topology configurations. The popular SIMP method [41], for example, models the search space as discrete functions on the discretized design domain. In other words, each point represents the "pixel" of the desired blueprint of the optimal design. As a consequence, a good resolution of the design may require a large number of pixels, and these pixels model both void and solid regions.

Similarly to our computational methods, natural systems are also restricted to a finite encoding: the DNA. However, natural systems have devised a strikingly different solution to the finitude problem, where the DNA encodes a developmental program that when "compiled and executed" performs a sequence of tasks that develops the final structure in stages. The results are patterned, complex, and multi-scaled structures that perform multiple task functions and are generically resistant to damage.

The goal of this research will be to develop a cellular proliferation process that mimics the developmental stages of natural organisms. These laws can be evolved to respond to desired requirements, and thus be used to search for high-performing engineering layouts.

1. ONE DIMENSIONAL MODEL

We first study a simple case in order to understand how it is possible to model such a biological process, defining control inputs and basic rules that will be developed further on. Our initial assumption is that the geometric configuration of the cells is a ring of at least 3 cells. For the ring of cells, the topology is unaffected, as only the radius increases. The model is a control system that will predict the dynamic distribution of fractones (and attached cells) and their contribution to the morphogenesis process. The system will be modeled as a control system to incorporate dynamic changes in the distribution of fractones among the cells. In general, the state space of our control system represents the concentrations of a given number of growth factors at a precise location in a given configuration of cells. Mathematically, these systems are described by a differential equation of the form:

$$\dot{x}(t) = f(x(t), u(t)), \quad x(t) \in M \tag{1.1}$$

where M is a n-dimensional smooth manifold, x describes the state of the system and $u : [0,T] \to U \subset \mathbb{R}^m$ is a measurable bounded function called the control. Despite the fact that the field of control theory covers such a broad range, the biological process that we are analyzing presents a completely new challenge from the control theory point of view. We are primarily concerned with the affine control system:

$$\dot{x}(t) = F^0(x(t)) + \sum_{j=1}^{m} F^j(x(t))u(t), \quad x(t) \in M \tag{1.2}$$

where the vector field F^0 is referred to as the drift and the F^js are referred to as the control vector fields (m represents the number of available inputs, in particular if $m < n$ we say that the system is underactuated). Let us consider the state space of our control system to be the concentrations of a given number of growth factors at a precise location in a given configuration of cells. The drift vector field will represent the diffusion property of the growth factors under the condition that no fractone is active

while the control vector fields represent the impact that a fractone will have on the diffusion process once it is activated. The spatial distribution of the fractones is governed by the control function:

$$u_i(t) = \begin{cases} 0 & \text{if fractone inactive} \\ 1 & \text{if fractone active} \end{cases} \quad for\ 1 \le i \le m \tag{1.3}$$

Assume that we have k growth factors diffusing among the cells; we call them X^k. Each growth factor has its own diffusion rate that will be denoted by $\nu_k > 0$ and X_i^k represents the concentration of the growth factor X^k in the ith–cell. Note that 0th–cell is synonymous with the Nth–cell, where N represents the total number of cells. Now, we describe the system for a single growth factor. The component i of the drift vector field $F^{k,0}(X^k(t))$ is:

$$F^{k,0}(X^k(t)) = \nu_k(X_{i+1}^k - 2X_i^k + X_{i-1}^k) \tag{1.4}$$

This equation comes from Turing, and is modified to reflect that there are no cross-reaction terms (since the GFs are non-interacting) and the presence of a diffusion constant for each respective growth factor. The system $\dot{X}^k(t) = F^{k,0}(X^k(t))$ represents pure diffusion.

Now, as $t \to \infty$, such a system tends to the steady state solution in which the concentration of growth factor is identical in each cell. However, once a fractone associated to the ith-cell is activated, the diffusion process is perturbed; there is diffusion from the neighboring cells to the ith-cell but diffusion from the ith-cell to its neighboring cells is prevented. In other words, the fractone associated to the ith-cell acts as a captor of growth factor. In terms of the equations describing the system, when the fractone associated to the ith-cell is activated, only the component u_i of the control is turned on (taking the value 1) and the control vector field $F^{k,i}(X^k(t))$ describes the new diffusion process. By construction, $F^{k,i}(X^k(t))$ only affects the diffusion of the $(i-1)^{th}$, ith, and $(i+1)^{th}$-cells. Now, we introduce the exchanging function that dictates whether neighboring cells give growth factor to one another by:

$$H_{st}(t) = H(X_s^k(t) - X_t^k(t))(X_s^k(t) - X_t^k(t)) \tag{1.5}$$

where we define:

$$H(z)=\begin{cases}0, \ if \ z \le 0\\ 1, \ if \ z > 0\end{cases} \tag{1.6}$$

With these notations, we have:

$$\begin{aligned}F_i^{k,i}(X^k(t)) &= \nu_k(H_{i+1,i}+H_{i-1,i}-F^{k,0}(X^k(t)))\\ F_{i-1}^{k,i}(X^k(t)) &= \nu_k(H_{i-1,i}-X_i^k+X_{i-1}^k)\\ F_{i+1}^{k,i}(X^k(t)) &= \nu_k(H_{i+1,i}-X_i^k+X_{i+1}^k)\end{aligned} \tag{1.7}$$

and all the other components of the control vector field $F^{k,i}(X^k(t))$ are zero. If we consider multiple growth factors diffusing among the cellular structure, we must take them into account via superposition of the system and implementation of a hierarchical system to describe the affinity of a given fractone with a certain type of growth factor. This adds complexity to the system, but it is a straightforward extension.

From the point of view of control theory, system (1.2) falls into the classical theory of control systems since it is affine and fully actuated (a fractone can potentially be activated in any cell). All the components of the control are piecewise constant functions that take their values from the set {0, 1} and, given an initial distribution of fractones, it is trivial to produce a control to reach a prescribed final distribution of cells. However, to achieve our goal, we must develop a more realistic model to incorporate the activation of the growth factors that will dictate the multiplication of cells.

To refine the model we've developed thus far, we assume that once a given concentration for the growth factor X^k is reached at a fractone (or, equivalently, a captor), it releases the information to the attached cell to duplicate, and the concentration of growth factor in the cell drops to a lower amount. When this situation manifests, the number of cells in the ring grows from N to N+1. This implies that the state space on which our biological control system is defined is dynamic, as its dimension transforms with the cells duplication. Based on how we perceive the system to function, the control system that models it is as follows:

$$\dot{x}(t)=F^0(x(t))+\sum_{j=1}^{N(t)}F^j(x(t))u(t), \quad x(t)\in M \tag{1.8}$$

where M(t) is now a space whose dimension and topology varies with time. In a simplified way, this corresponds to saying that the number of cells grows, which is reflected in the equation by the introduction of N(t). Also, the domain of control now varies since fractones can potentially become active in the new cells.

2. TWO DIMENSIONAL MODEL

We need to define the relevant components for the biological process under consideration, and their discretization: the ambient space, the cells, the bones and the fractones.

2.1 Discretization of the problem

The ambient space in which the morphogenic events take place is assumed to be a compact subset of $\mathbb{R}^2$ and, for simplicity, we assume the ambient space is fixed. We denote by M a discretization of the ambient space (using for instance discretization by dilatation or Hausdorff discretization, see [45] and Figure 3).

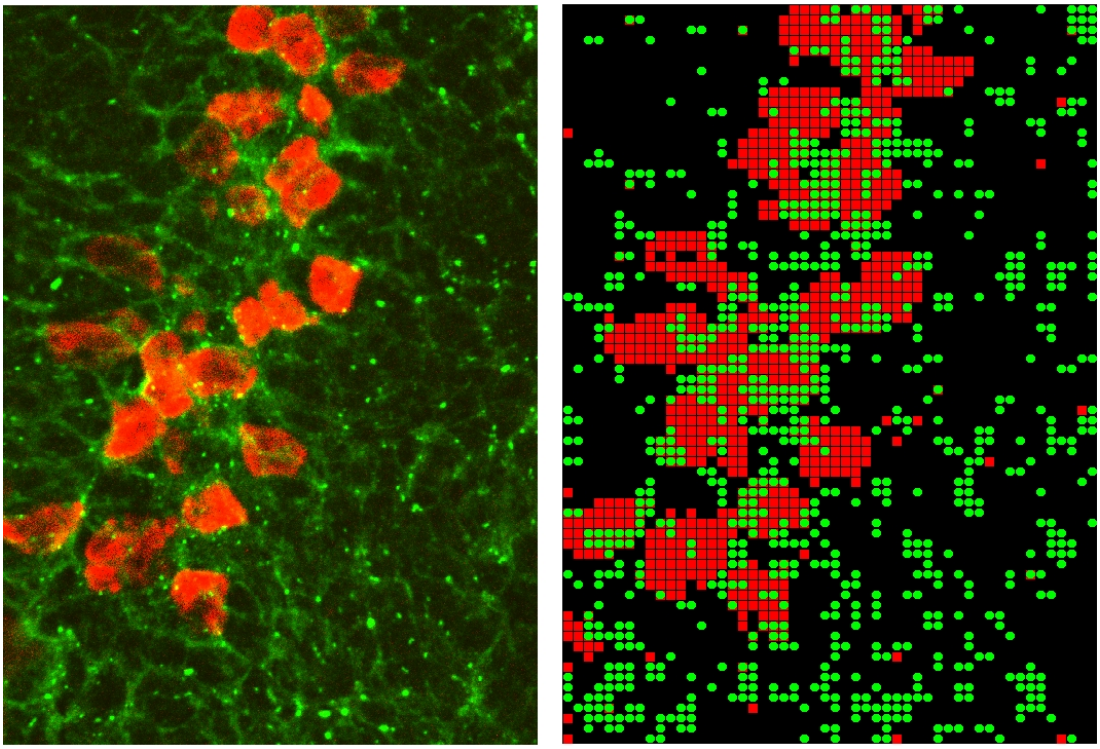

Figure 3 - Discretisation of a fractone map

So, in the sequel, M is identified to a subset of $\mathbb{Z}^2$. The precision of the discretization is initially set by the user but eventually will be determined by the experimental biological maps. To avoid any confusion with the biological cells, in the rest of this thesis, we call a cell of our discretization a unit and we identify each unit to an ordered pair of integer (i, j). The origin unit of our discretization is chosen arbitrarily and will be identified to $(0,0)$. We assume that the boundary of the ambient space in which the biological process takes place is fixed but our definitions allow for boundaries that vary with time as well.

For simplicity will consider a rectangular ambient space, but we can easily modify its shape by modeling bones. Intuitively, in our discretization, a bone will be modeled as a region not accessible to our system: we can imagine it as an hole (inside the ambient space) or a wall (if it changes the boundary of the ambient space). Referring to the proper definition of M, bones are useful to design the shape of the ambient space but once we get the desired conformation, bones will not show up in our model. There is no restriction in the use of bones because they are defined unit by unit, in order to create any shape needed.

The morphogenic event will start from an initial configuration of cells immerged in what we call the ambient space. Growth factors diffuse within the ambient space but can't go through cells. A cell border is modeled as a wall for the growth factors that are outside the cell but we'll see further on that the cell will be able to produce growth factors that will diffuse in the ambient space. We assume that the space between the cells account for 20% of the total space occupied by the cells. This is reflected in our discretization by representing a cell as a square composed of 81 units (i.e. a 9 by 9 square) [2], while the "in-between cells" space is represented by single unit-rows and unit-columns. Notice that at this stage of the work it is an arbitrary choice and it will be straightforward to adjust it to reflect the observations from the experimental maps. We assume the cells to be vertically and horizontally aligned.

[2] From a purely theoretical point of view, there are many ways that we can represent the cells in the ambient space. Indeed, we can make the assumption that they are all circular and have the same dimension or that their shape differs in size and form. Notice that, from a practical point of view, the shape and size of the cells of the initial configurations will be given by the experimental map and its discretization. To write the dynamic model of our biological process we only assume that the size and shape of all cells are identical.

Finally, in our discretization, a fractone is represented as one unit. Growth factors are attracted by fractones and are stored in them.

The three important spaces to take into account into our dynamical system are: the space filled with cells, the space in which the growth factors diffuse and finally the space filled with the fractones. Those objects are defined in the following definitions.
We denote by $Cell(t)$ the configuration of cells in the ambient space at a given time t, and we call it the cell space. It is a closed subset of the ambient space and is identified in the sequel to a subset of M.
The diffusion space at time t, denoted by $Diff(t)$, represents the space in which growth factors are diffusing. It is the complement of the cell space in the ambient space and its discretization is identified to $M \setminus Cell(t)$. At each time t, the diffusion space is split into two components, the free diffusion space $Free(t)$ where the growth factors diffuse freely, and the fractone space, $Fract(t)$, where the diffusion is perturbed. The data of $Cell(t)$, $Free(t)$ and $Fract(t)$ forms what we call the configuration space at time t, and we denote it by $Conf(t)$.
Note that $M = Cell(t) \cup Diff(t)$ and $Diff(t) = Fract(t) \cup Free(t)$.
Let $M(t)$ be one of the spaces defined above. We define the dimension of the space M at time t as the number of indices (i, j) such that $(i, j) \in M(t)$ where $M(t)$ has been identified to its discretization.

Topologically, we can interpret the above definitions as follows: we can visualize the configuration space at a given time t as a compact subset of $\mathbb{R}^2$ with holes depicted by the cells. On a given discretization of this topological space (varying with time), we will model the diffusion of growth factors (which is perturbed at the location of a fractone). Finally, we will incorporate into our model the mechanisms that allows duplication of cells named mitosis.

An example of how the discretization process takes place is shown from Figure 4 to Figure 7, where we can see the diffusion space (highlighted by the grid showing free units) of complex shape, thank to the use of bones, plus cells (in blue) and fractones (green units).

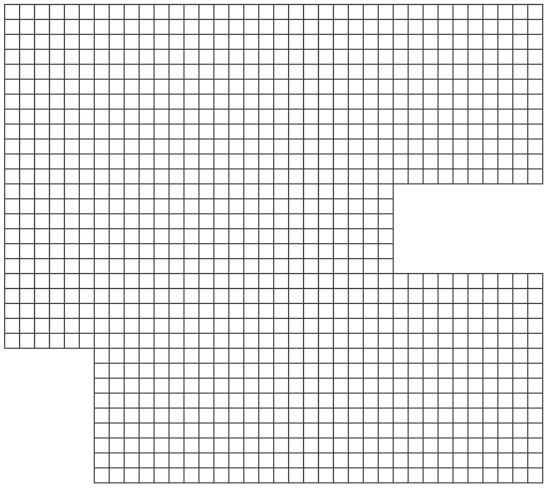

Figure 4 - Discretization: Free(t)

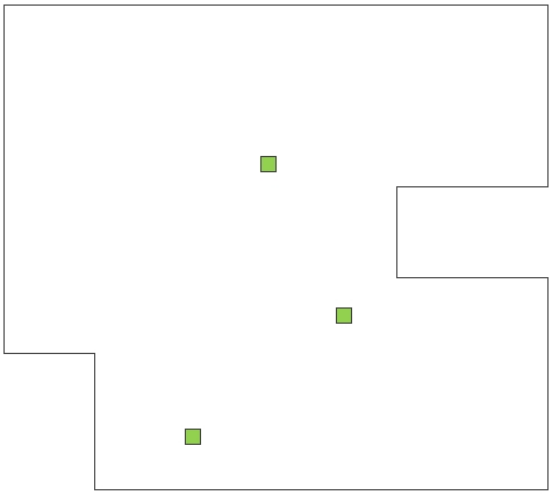

Figure 5 - Discretization: Fract(t)

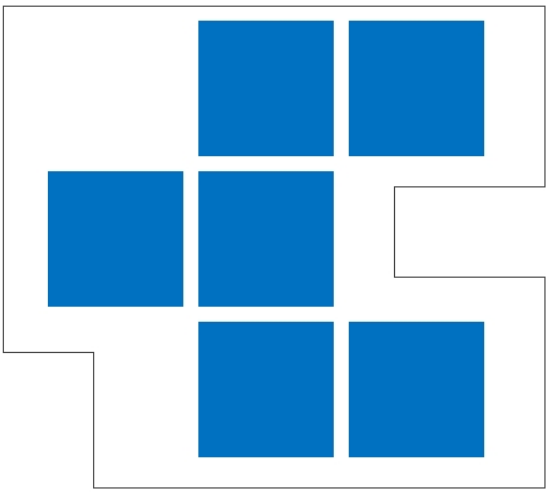

Figure 6 - Discretization: Cell(t)

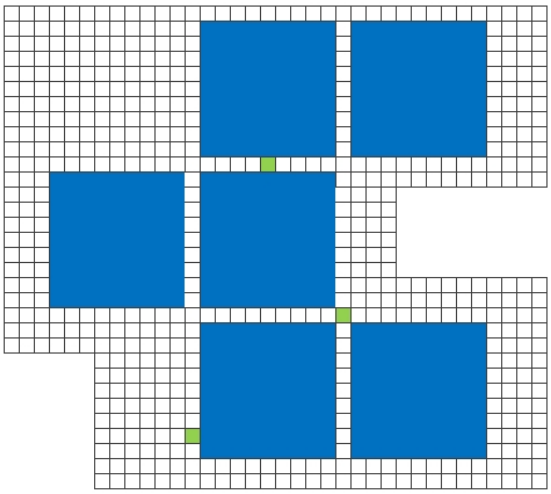

Figure 7 - Discretization: Conf(t)

2.2 Diffusion of growth factor

For simplicity, we assume the diffusion of a unique type of growth factor and equal sensitivity of the fractones with respect to that growth factor. However, our model will be developed such that expanding to several types of growth factors and varying fractone sensitivity to respective growth factors can be added in a straightforward way. The state space is defined at each time t as the concentration of growth factor in each unit of our discretization of the diffusion space $Diff(t)$. We denote the state space by

$M(t)$. More precisely, since there is a one-to-one correspondence between units and ordered pairs of integer, we have:

DEFINITION - Let $(i, j) \in Diff(t)$. At each time t, we introduce the concentration of growth factor in unit (i, j) that we denote by $X_{i,j}(t)$. The state space $M(t)$ at time t is then $M(t) = \mathbb{R}_{\geq 0}^{\dim(Diff(t))}$.

Assume at first that there is no cells and no fractones. Therefore, the growth factors diffuse freely in the ambient space. We denote by ν the diffusion parameter associated to the considered growth factor, and in order to accurately describe the mechanism we introduce $\Delta = \{(0,1),(0,-1),(1,0),(-1,0)\}$.

Pure dissipation is then described by:

$$\dot{X}(t) = F^0(X(t)) \tag{2.1}$$

where the components of $X(t)$ are given by $X_{i,j}(t)$ which represents the quantity of growth factor in unit (i, j) at time t as described chapter 1, and, assuming diffusion occurs between a unit (i, j) and its four neighbors, we have:

$$\dot{X}_{i,j}(t) = \nu \sum_{(k,l)\notin\Delta} (X_{i+k,j+l}(t) - X_{i,j}(t)) \tag{2.2}$$

for $(i, j) \in Diff(t)$, see Figure 8.

Assume now that a cell forms in the ambient space. The cell therefore becomes an obstacle to the diffusion process. Mathematically, rather than looking at a cell as an obstacle, we identify the cell to a hole in a topological space. The hole, depicting the location of the cell, insures that the diffusion of the growth factor takes place in the diffusion space only. By doing so, we do not have to perturb the diffusion process, instead we continuously modify the topological space in which the diffusion process takes place.

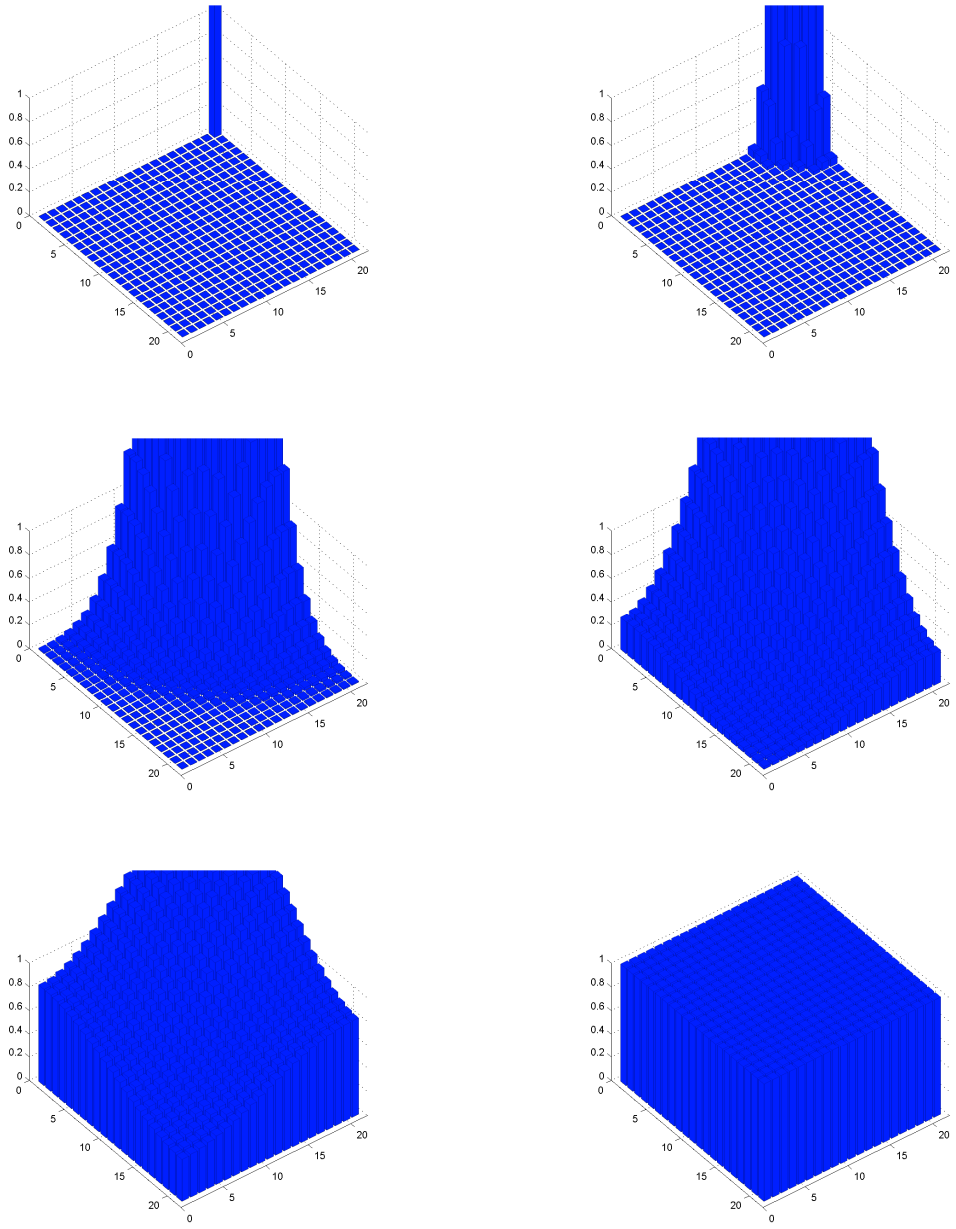

Figure 8 - Free diffusion

Let us describe the new state space on which the diffusion process takes place. Assume the cell is centered at unit (a,b). This means that at the time t at which the cell formed, the diffusion space $Diff(t) = I_t \times J_t$ transforms into a new free diffusion space $I_t \times J_t$ from $I_t \times J_t \setminus \left(\{a-4,\cdots,a+4\} \times \{b-4,\cdots,b+4\}\right)$,we assume it is instantaneous with no loss of generality. Notice that, since several cells might be forming at the same

time, the topological changes in the configuration space will reflect all the created holes. We then have:

$$\dot{X}_{i,j}(t) = \nu \sum_{\substack{(k,l)\in\Delta \\ (i+k,j+l)\in Diff(t)}} (X_{i+k,j+l}(t) - X_{i,j}(t)) \tag{2.3}$$

for $(i, j) \in Diff(t)$.

Finally, we need to model how fractones perturb the diffusion. As mentioned before, a fractone is represented as a one unit (i, j) of our discretization. The hypothesis is that the fractones store the quantity of growth factors that they capture, and that this quantity becomes unavailable to the diffusion process. To reflect the biological hypothesis that fractones are produced and then disappear, we introduce the following definitions.

DEFINITION - To each unit (i, j) we associate what we call a passive fractone. A passive fractone at time t belongs to $Free(t)$. An active fractone at time t is defined as a unit that belongs to the set $Fract(t)$. An active fractone is one that acts as a captor for the diffusion process.

The biological translation of this definition goes as follow. A passive fractone corresponds to the situation such that either no fractone is associated to the unit or one is currently produced but is not yet part of the biological process. In other words, in our representation it can be seen that $Free(t)$ is the set of passive fractones at time t. An active fractone is one that acts as a captor for the diffusion process.

Assume now that there is an active fractone (i, j). Then there is perturbation to the diffusion process as follows. We introduce a control function $u(t) = (u_{i,j}(t)) \in \{0,1\}^{I_t \times J_t}$ defined on a time interval $[0,T]$, with T representing the duration of the cascade of morphogenic events under study. When a fractone is active at time t, the component $u_{i,j}(t)$ of the control is turned on to 1 while it is set to zero for a passive fractone. The active fractone store the current quantity of growth factors available in unit (i, j) and acts as captor for the diffusion process. In other words, diffusion from an unit

$(i, j) \in Fract(t)$ to its neighbors is prevented. To represent this perturbed diffusion process, we define a control system:

$$\dot{X}(t) = F^0\big(X(t)\big) + \sum_{(i,j)\in Diff\,(t)} F^{(i,j)}\big(X(t)\big)\cdot u_{(i,j)}(t) \tag{2.4}$$

where $X(t)$ is the state variable and denotes the concentration of growth factor in the diffusion space $Diff\,(t) = I_t \times J_t$ at time t, the drift vector field F^0 is given by (2.3) and represents the regular diffusion of growth factors taking place in the free diffusion space, and finally the control vector fields perturb the regular diffusion to account for the possible presence of active fractones. More precisely, we have under the assumption that (i, j) is an active fractone:

$$F_{i,j}^{(i,j)}\big(X(t)\big) = \nu \cdot \sum_{\substack{(k,l)\in\Delta \\ (i+k,\,j+l)\in Diff\,(t)}} X_{i,j}(t) \tag{2.5}$$

$$F_{i+k,\,j+l}^{(i,j)}\big(X(t)\big) = -\nu \cdot X_{i,j}(t), \quad for \begin{cases} (k,l) \in \Delta \\ (i+k,\, j+l) \in Diff\,(t) \end{cases} \tag{2.6}$$

Those equations reflect the fact that the quantity of growth factor in an active fractone become invisible to the diffusion process. Once the stored quantity reaches a given threshold, the fractone signals to the cells that mitosis can occur. Moreover, a key element in our hypothesis is that the spatial distribution of fractone varies through the sequence of morphogenic events. The role of the function $u(\cdot)$ introduced in (2.4) is precisely to control the location and activation of the fractones.

DEFINITION - An admissible control is a measurable function $u : [0,T] \to \{0,1\}^{n(t)}$ where T represents the duration of the morphogenic event under study, and $n(t)$ is the number of pairs included in $I_t \times J_t$.

In Figure 9, we represent a simulation of the perturbed diffusion process when cells and fractones exist in the ambient space. The initial distribution of growth factor is a single source (not to scale) as seen in the initial image in the upper corner above the cell, while the fractone is located near the bottom corner in green. The growth factors

diffuse through the free space to eventually be captured by the fractone in the last image.

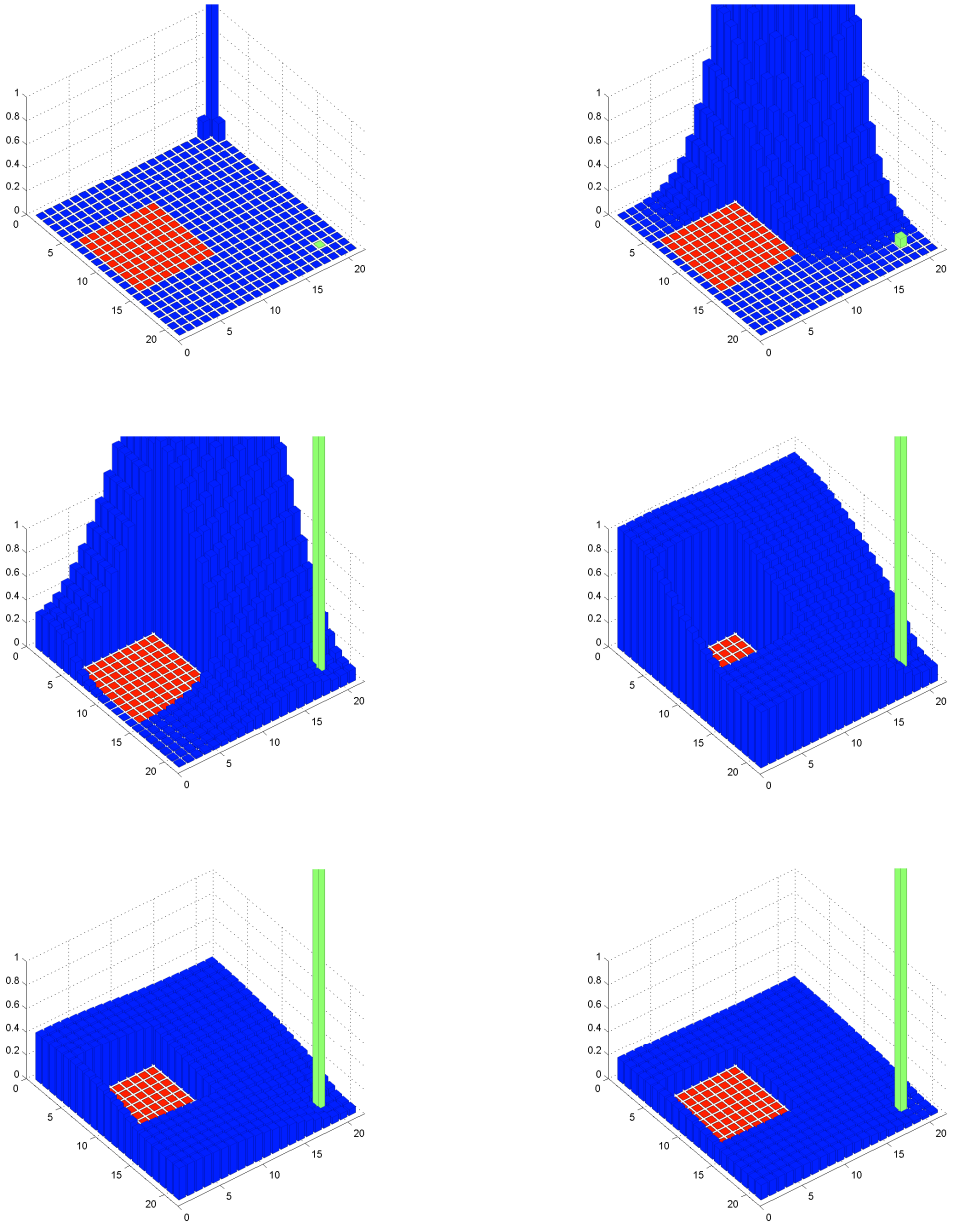

Figure 9 - Perturbed diffusion

2.3 Mitosis

As mentioned in the introduction, growth factors are regularly produced by the biological cells and then are diffusing freely in the available extra-cellular space. When the growth factor is significantly close to an active fractone, said fractone captures and concentrates the growth factor. Once the concentration of growth factor reaches a significant value, the fractone gives the order to its associated cell to undergo mitosis. In reality, the time for a cell to undergo mitosis is approximately four hours. However, by the time mitosis actually occurs, the fractone may have relocated. What is interesting is that the previous location of a fractone has been shown to be the location of new cells after the next morphogenic event. Due to this correlation, it is clear that the spatial distribution of fractones dictates the location of future morphogenic events, hence the fractones are the obvious choice to represent the controls in our system. One may argue that the reality does not match the model in that there is a time lapse in which the fractones may or may not move, and the cell undergoes mitosis. To alleviate this problem, the model is so that mitosis occurs instantaneously once an order has been issued by a fractone, and that fractone movement is also instantaneous in what we associate every available unit in $Free(t)$ with a fractone, and that "*moving*" a fractone is equivalent to changing the control from 1 to 0 in one location (making this fractone inactive) and vice-versa in another location (making this fractone active). To equivalently describe this process mathematically, we state that the spatial distribution of the fractones and the concentrations of freely-diffusing growth factors dictate the location and appearance of holes (i.e. cells) in the configuration space.

Now that mitosis is occurring, a natural question arises: when a cell undergoes mitosis, how does the existing mass of cells deforms? The deformation of the mass of cells undergoing morphogenic events is extremely complex. Indeed, it involves many different criteria to take into account as well as forces to optimize. Our goal in this paper is to state and start analyzing some control problems formulated in a new setting rather than to produce the most accurate simulation of the biological process which would render such a complex system that an analytic study could not be conducted. Therefore, our criterion for the deformation of the mass of cell is based on the

minimization of a given distance function, based on the assumption that the mass of cell is optimizing its shape by prioritizing compactness. It is clear that we can create a slender shape, for instance, acting on the control inputs.

We assume in the sequel that we have a distance function, denoted by d, defined on the set of ordered pairs of integers. More precisely, for each $a=(a_1,a_2), b=(b_1,b_2)\in\mathbb{Z}\times\mathbb{Z}$, the distance between a and b is well defined by the positive real number $d(a,b)$

When mitosis occurs at a given time t, the configuration space $Conf(t)$ undergoes a topological change. Indeed, with new cells forming, they become additional holes in the ambient space, and while the dimension of $Free(t)$ decreases, the dimension of $Cell(t)$ increases. To accommodate for the formation of new cells, $Cell(t)$ has to deform accordingly to a prescribed algorithm. Assume unit (i, j) represents an active fractone and we denote by C_i the associated cells (under our current assumptions a fractone can be linked up to four cells: $i=\{1\ldots4\}$). Since we assume all cells rigid and of equal shape, we can identify a biological cell to a single unit of our discretization.

Each cell can be identified to its middle unit denoted here by (a,b) and we can write $C(a,b)$. The deformation algorithm is defined as to preferentially deform the current mass of cells in the direction of the closest empty space in a clockwise orientation as starting from angle zero (as referenced by an axis superimposed on the center of the "*mother*" cell). More precisely, assume $C(a,b)$ duplicates. The algorithm looks incrementally for the closest unit $(i, j)\in Free(t)$ to (a,b) (based on the chosen distance d) such that (i, j) can be identified to a cell. Since more than one unit identified to a cell can be at the same distance from (a,b), we need to use a selection algorithm. There are many ways to select among those units; it could even arbitrarily be determined by the computer.

First, we need to introduce a notion of distance: let $\alpha_1=(a_1,b_1)$, $\alpha_2=(a_2,b_2)\in\mathbb{Z}\times\mathbb{Z}$, we consider the Euclidean distance:

$$d_E(\alpha_1,\alpha_2)=\sqrt{|a_1-a_2|^2+|b_1-b_2|^2} \tag{2.7}$$

As it was explained above, we assume that each cell is identified to its middle unit of its discretization. It is therefore understood that $C=(a,b)=\{(i,j)\in Cell(t);\ a-4\le i\le a+4,\ b-4\le j\le b+4\}$. Let $C_i=(a_i,b_i)$, $i=1,2$ be two biological cells. Therefore, since between two cells we have a unit-wide channel, then $a_1=a_2 \bmod 10$ and $b_1=b_2 \bmod 10$ and $d_E(C_1,C_2)\in\left\{10\sqrt{n^2+m^2}\mid n,m\in\mathbb{Z}\right\}$. It follows that the deformation algorithm will search for the closest units in *Free*(*t*) that are at distances of the form $10\sqrt{n^2+m^2}$ from the cell undergoing mitosis. Notice that, given a cell C, the closest units multiples of 10 from C are at a distance 1 (i.e. $(n,m)=(0,1)$ or $(1,0)$), and there are 4 of them. The next closest units of 10 are at a distance $\sqrt{2}$,and there are also 4 of them. Table 2 lists some of the possible distances (divided by 10 in the table). The pattern is very clear and only one half of one quadrant is displayed since it is symmetrical with respect to the other quadrants, and the table is symmetrical about its diagonal.

As we'll see further on, it is straightforward to relax the assumption that the distance between two connected cells is equal to 10 units or, in other words, that between two cells we have a unit-wide channel. In order to prevent confusion, we define

$$D=d_E \bmod \delta \tag{2.8}$$

Where δ is the distance between the connected cells (by now we have $\delta=10$)

0	1	2	3	4	5	6	7	8	9	10
1	$\sqrt{2}$									
2	$\sqrt{5}$	$\sqrt{8}$								
3	$\sqrt{10}$	$\sqrt{13}$	$\sqrt{18}$							
4	$\sqrt{17}$	$\sqrt{20}$	$\sqrt{25}$	$\sqrt{32}$						
5	$\sqrt{26}$	$\sqrt{29}$	$\sqrt{34}$	$\sqrt{41}$	$\sqrt{50}$					
6	$\sqrt{37}$	$\sqrt{40}$	$\sqrt{45}$	$\sqrt{52}$	$\sqrt{61}$	$\sqrt{72}$				
7	$\sqrt{50}$	$\sqrt{53}$	$\sqrt{58}$	$\sqrt{65}$	$\sqrt{74}$	$\sqrt{85}$	$\sqrt{98}$			
8	$\sqrt{65}$	$\sqrt{68}$	$\sqrt{73}$	$\sqrt{80}$	$\sqrt{89}$	$\sqrt{100}$	$\sqrt{113}$	$\sqrt{128}$		
9	$\sqrt{82}$	$\sqrt{85}$	$\sqrt{90}$	$\sqrt{97}$	$\sqrt{106}$	$\sqrt{117}$	$\sqrt{130}$	$\sqrt{145}$	$\sqrt{162}$	
10	$\sqrt{101}$	$\sqrt{104}$	$\sqrt{109}$	$\sqrt{116}$	$\sqrt{125}$	$\sqrt{136}$	$\sqrt{149}$	$\sqrt{164}$	$\sqrt{181}$	$\sqrt{200}$

Table 2 - D: distance distribution as measured from the "*mother*" cell

We have three options:

a) 12 possible units if D is an integer that is the hypotenuse of a Pythagorean triple[3]
b) 8 possible units if D is not along a diagonal or an axis
c) 4 possible units if D is on a diagonal or an axis, and is not the hypotenuse of a Pythagorean triple

[3] A Pythagorean triple consists of three positive integers a, b, and c, such that $a^2 + b^2 = c^2$. It is easy to verify from Table 2 that the Pythagorean triple (3,4,5) returns 12 units: 4 on the axis, such as (5,0) and 8 from (±3, ±4) and (±4, ±3)

As a resume of the notions of distance that we'll be using, we have:

1) Distance in units: d
2) Euclidean notion of distance: d_E
3) Distance between cells: D

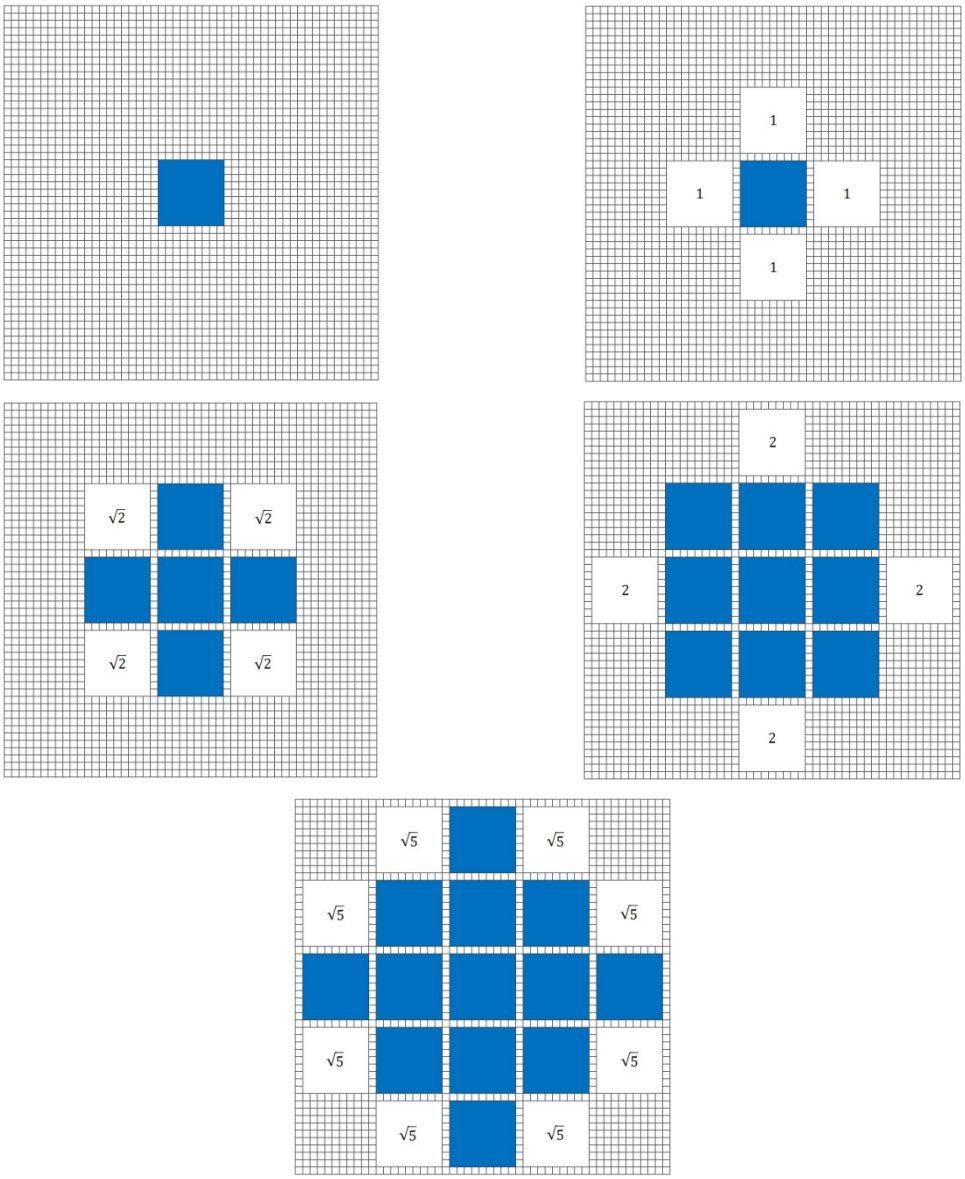

Figure 10 - Distance distribution: an example

Now, consider for simplicity a single cell undergoing mitosis. The deformation algorithm is defined as to preferentially deform the current mass of cells in the direction

of empty space in a clockwise orientation as starting from angle zero (as referenced by an axis superimposed on the center of the "*mother*" cell). More precisely, it looks incrementally for the closest unit to (i, j) that belongs to $Free(t)$. Once such a unit is detected, the deformation occurs.

Units at a same distance from (i, j) are selected in the following order. The linear component distances, respectively, from a cell undergoing mitosis to a location toward which the mass can deform are $i_l - i_0$ and $j_l - j_0$, for all l, where l represents the number of possible locations at a given distance and (i_0, j_0) represents the center of the cell undergoing mitosis. The algorithm looks first for a unit in $Free(t)$ such that $j_l - j_0 \leq 0$ and chooses preferentially the max $\max\{i_l\}$. If no such unit is found, the algorithm searches for a unit in $Free(t)$ such that $j_l - j_0 > 0$, and chooses preferentially the $\min\{i_l\}$.

In the case of multiple cells undergoing mitosis, we made the assumption that there is a hierarchical rule to define which cell duplicates first: we associate to each cell an age and the oldest duplicates first (intuitively it is easy to define a scale of ages as new cells are born, and for those cells that belong to $Cell(t) \mid t = 0$ such hierarchy will be defined following the order in which the user inputs cells positions). Note that this is an arbitrary choice, that can be straightforwardly modified whenever a biological evidence dictates a more consistent rule.

Finally, if a fractone is not associate to any cell it will keep storing growth factors until a cell is close enough. At this point mitosis will occur immediately.

In Figure 11, we display a sequence of morphogenic events to illustrate how our deformation algorithm works. Notice that, as explained before and shown in this example, it is possible to use a discretization algorithm that associates to cells a circle inscribed in a 9 by 9 square without loss of generality. Starting from a unit cell and a single fractone that can be associated up to two cells (it is not placed at a cell corner), the sequence of images illustrate the deformation algorithm as duplication of the cell associated to the fractone occur. If we choose the origin such that the center of the initial cell is at $(0, 0)$. we have that the initial cell space (Figure 11,1) is

$\{(i, j) \in \mathbb{Z} \times \mathbb{Z} \mid -4 \le i \le 4, -4 \le j \le 4\}$, and the final cellspace (Figure 11,11) is $\{(i, j) \in \mathbb{Z} \times \mathbb{Z} \mid -26 \le i \le 26, -26 \le j \le 26\} \setminus$
$\{(i, j) \mid i \in \{-6, -5, 5, 6, 16, 17\}, j \in \{-6, -5, 5, 6, 16, 17\}\}$.

Note that the ambient space is limited and gets filled up by last duplication.

When a cell undergoes mitosis and the distance algorithm has chosen a position in $Free(t)$ for $Cell(t)$ to deform toward (let us refer to this closest selected unit at a distance D as (c, d)), the growth factor present in the space must move in order to make room for the deformed mass of cells. Hence, the algorithm for redistribution of GF occurs as follows:

1) it calculates the sum of the GF present in the space associated to a cell centered in unit $C = (c, d)$ where the mass of cells will deform toward, i.e.

$$\sum_{k,l=-4}^{4} X_{c+k,d+l}(t) \tag{2.9}$$

2) deforms $Cell(t)$ such that $(c, d) \in Cell(t)$.
3) counts the number of units in $Free(t) \cup Fract(t)$ that are at a distance $d \le 8$ from (c, d).
4) distributes 70% of the sum from (1) evenly in each unit from (3).
5) counts the number of units in $Free(t) \cup Fract(t)$ at a distance $8 \le d \le 11$ from (c, d).
6) distributes the remaining 30% of the sum from (1) evenly in each unit from (5).

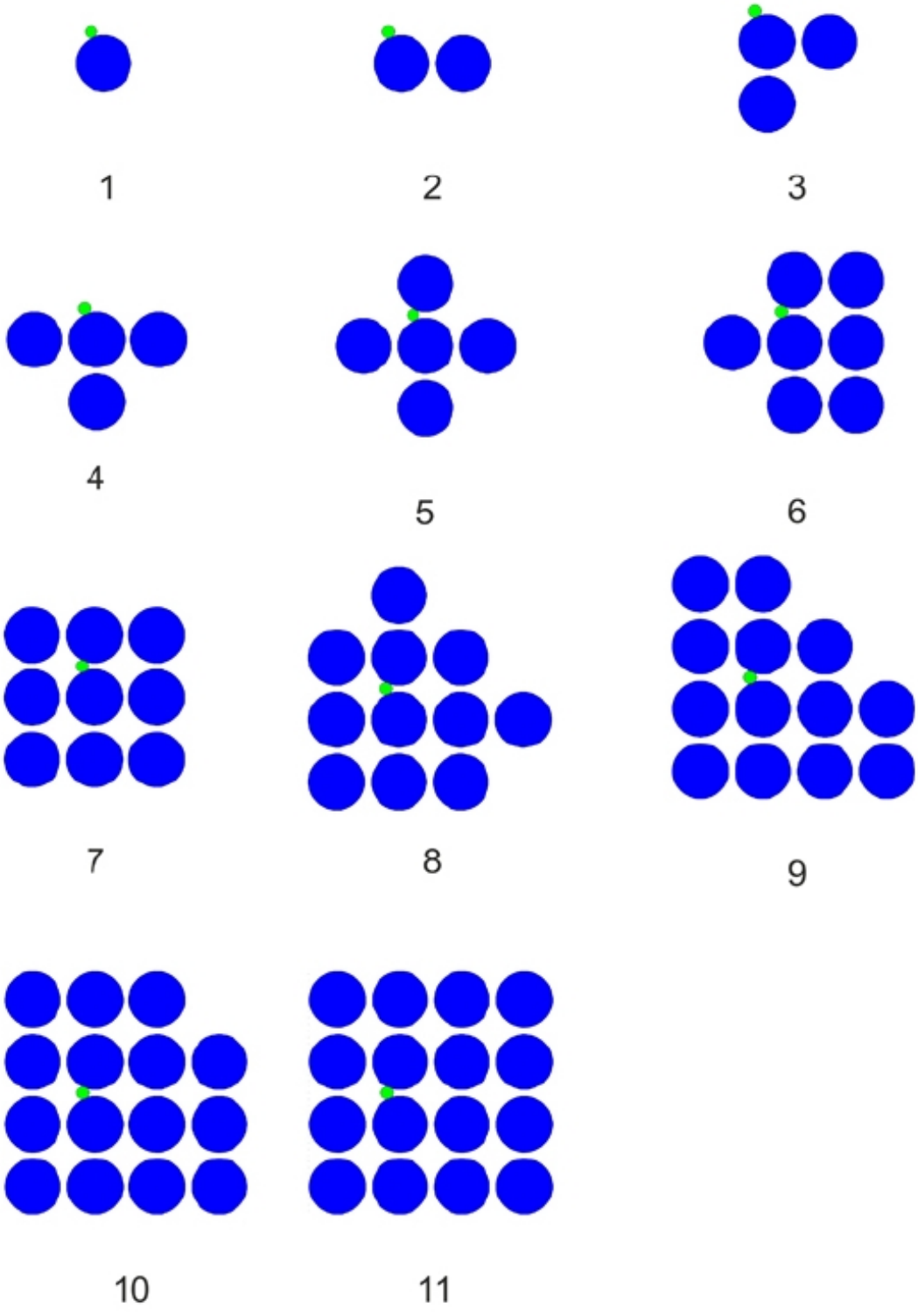

Figure 11 - Deformation algorithm

From the details thus far, we can glean the criteria that guide the system from one topological space to the next:

a) in the absence of cell production of GF, the initial concentration of growth factor(s) dictate how many times mitosis can possibly occur (maximum number of cells, maximum number of configurations),
b) the group of cells arrangement(s) will dictate how GF is distributed throughout, thus determining possibility for mitosis,
c) the number of fractones present will determine the maximum change in dimension at any given time t,
d) the affinity of the individual fractone to a certain GF,
e) how often the cells, now producing GFs, do this and in what amounts,
f) the amount of any one GF required to initiate mitosis,
g) the "reset value" a fractone assumes post-mitosis, and
h) how many cells each individual fractone is associated with.

Following the mitosis algorithm defined above, we can generate a complex simulation with multiple active fractones involving several morphogenic events to reach the final desired configuration (Figure 12).

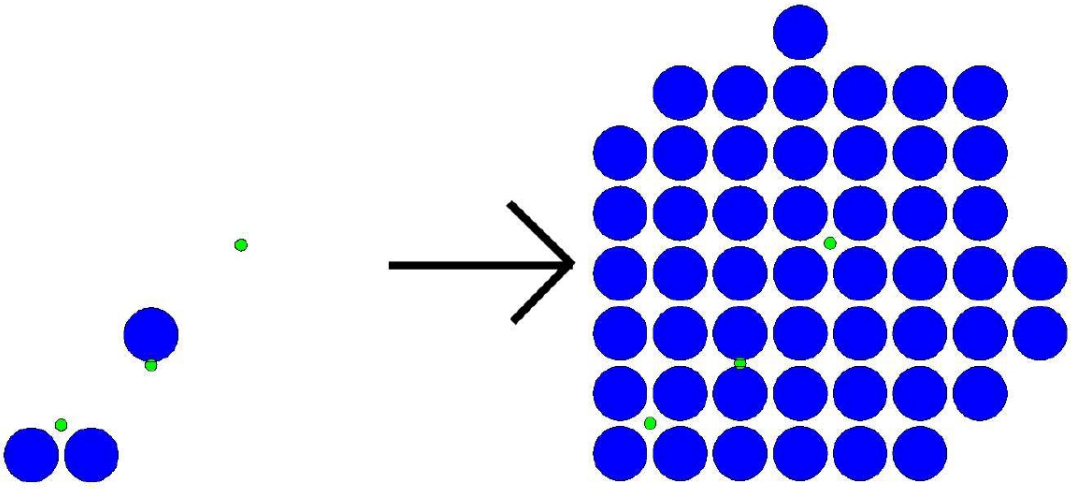

Figure 12 - First and last frame of a simulation with multiple cells and fractones

3. THEORETICAL QUESTIONS AND RESULTS

We can state our problem form a biological point of view:

PROBLEM α - Given an initial and final configuration of cells in a prescribed ambient space, determine an initial concentration of growth factors and a dynamic spatial distribution of fractones such that the mass of cells transforms from its initial configuration to its final configuration.

Let us now rephrase this using the mathematical definitions introduced previously. To summarize, the quantity of growth factor in each unit of our discretization is regulated through the following affine control system:

$$\dot{X}(t) = F^0\big(X(t)\big) + \sum_{(i,j)\in Diff(t)} F^{(i,j)}\big(X(t)\big)\cdot u_{(i,j)}(t), \quad X(t)\in M(t) \qquad (3.1)$$

where the state space $M(t) = \mathbb{R}_+^{\dim(Diff(t))}$ varies with time, the vector fields F^0, $F^{(i,j)}$ are given respectively by equations (2.3) and ((2.5),(2.6)), and such that $u(\cdot)$ is an admissible control. What is unusual in the considered problem with respect to traditional control problems is that the initial and final conditions are given in terms of $Cell(0)$ and $Cell(T)$ rather than in terms of $X(0)$ and $X(T)$. More precisely, we have:

PROBLEM α - Given A, $Cell(0)$ and $Cell(T)$, determine $X(0)$ and an admissible control $u(\cdot)$ such that $Cell(0)$ transforms into $Cell(T)$ under the evolution of system (3.1) and the prescribed rules for mitosis.

Notice that the admissible control is determined by the fractone set $Fract(t)$ at almost every time $t \in [0,T]$.

The key element in our model is the role played by the fractones as controllers. Under our hypothesis, they regulate cell's proliferation and differentiation. Growth factor intervenes in cell proliferation, but the fractones are the mechanism guiding and regulating GF. In our model, the production and diffusion of GF determines the time (or equivalently the order) at which the morphogenic events take place but it is the fractones that control the process. For instance, production of GF can always be altered such that a given active fractone will reach the GF threshold at a precise time. Moreover, the results presented in this section are based on having a unique active fractone at a time. Therefore, the diffusion and production of GF does not play any role in generating the morphogenic events (it only provides temporal information). For this reason, in this chapter, we consider the simplified problem where we neglect the GF diffusion and focus on how spatial distribution of fractones regulate cell proliferation. Once again, this is not a restrictive simplification and our results can be simulated using the complete model.

The results presented in this chapter are based on the assumptions made in chapter 2, in particular we consider the algorithm for deformation of the mass of cells described above. Now that the main problem has been stated, it is clear that the algorithm we have chosen for deforming $Cell(t)$ (the "clockwise" arrangement starting at angle zero) is arbitrary since any two spaces are equivalent if they are rotations of a factor of 90 degrees of each other. If we had picked a different algorithm (either in direction of cell deformation or starting angle from the mother cell), the two different algorithms would produce final configurations that were a rotation of $90 \cdot n$ degrees from each other (for $n \in \{1, 2, 3\}$).

The first two results deal with existence and uniqueness of solutions for our mathematical problem. Notice that cells are discretized as circles inscribed in a 9x9 square, without loss of generality as stated before.

3.1 Existence of solutions

As with any problem, one must check to see, for a given set of initial and final configurations, if there actually exist a solution to the problem, even in the simplest cases. For our problem, one can quickly produce a counterexample for which there is no "exact" solution. Of course, this is assuming that the initial configuration of cells is not one that arbitrarily leads to final configuration, such as the degenerate case in which $Conf(0) = Conf(T)$.

It is easy to envision a simple example for which a solution might not exist, as in Figure 13, if the initial configuration is that of one cell and one associated fractone, there is no way to produce the exact final configuration as shown. However, given the other initial configuration, it is clear that the final configuration in Figure 13 is a reachable configuration. This gives rise to a new level of complexity within the problem: the set of reachable final configurations (or, perhaps more appropriately, the set of non-reachable final configurations) as predetermined by the initial configuration. Even with this new point made, it is still obvious from our first counterexample that there does not exist for every set of given initial and final configurations a solution, i.e. a set of controls such that $Conf(0) \rightarrow Conf(T)$.

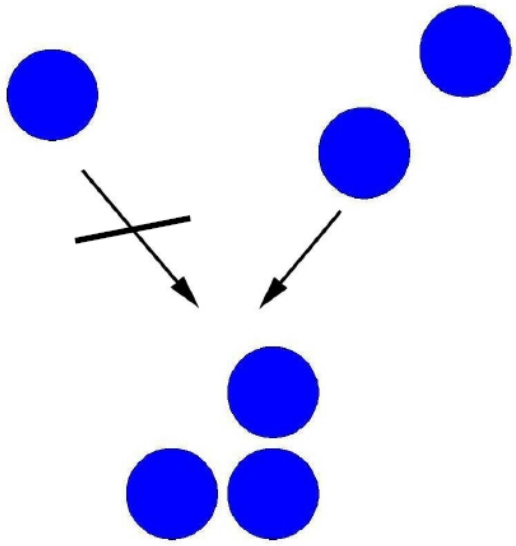

Figure 13 - Existence of solutions

3.2 Uniqueness of solutions

Given $Conf(0)$ and $Conf(T)$, suppose there exists a set of controls such that $Conf(0) \rightarrow Conf(T)$. Naturally, we should determine whether or not a solution to the problem is unique. As before, it is easy to choose an initial configuration and a final configuration such that the set of controls that guides the system is not unique. In Figure 14, we present an initial configuration and a final configuration for which the solution is clearly not unique. In this simulation, the fractone reaches the threshold to initiate mitosis from one level to the next lower level. Here, cells in red indicate the direction in which cell deformation occurred, fractones are green and cells in blue represent either static cells or "mother" cells.

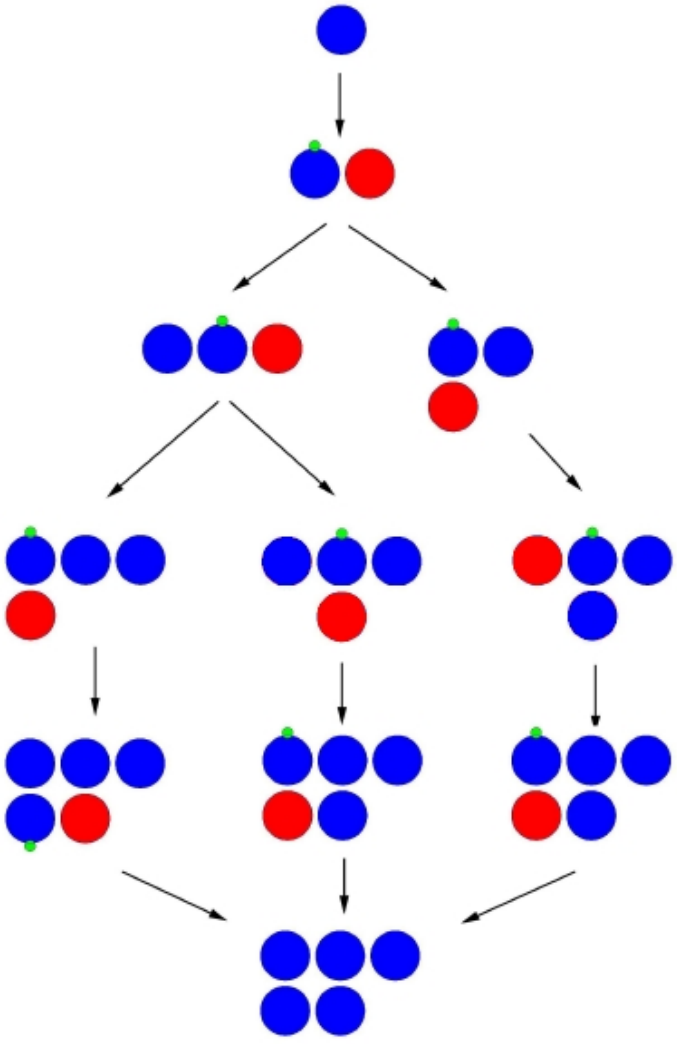

Figure 14 - Uniqueness of solutions

3.3 Notion of distance between configurations of cells

After stating the problem as above, we can attempt to formalize questions concerning the system. Indeed, as seen in Figure 13, there might not exist a solution to this problem for a given set of initial and final configurations. In this case, how do we modify the question? One solution is to introduce a notion of distance between configurations of cells and to ask how to reach a final configuration that is at the shortest distance from the desired one.

Before we can state some results we need to recall some definitions and introduce new ones. In order to measure how close two configurations of cells are from each other we use the Hausdorff distance. In the sequel, all spaces are identified to their corresponding discretization and a given ambient space A has been prescribed in which all the considered mass of cells live.

Given a cell space $Cell \subset A$, an element of $Cell$ corresponds to a biological cell. In our discretization, it is identified to a single unit (namely the center of the cell $C_a = (i_a, j_a) \in Cell$) representing the cell. Under the assumption that cells are horizontally and vertically aligned, we defined a notion of distance (see (2.7) and (2.8) for details) D:

$$D(C_a, C_b) = d_E \bmod \delta \tag{3.2}$$

where $C_a, C_b \in Cell$, d_E is the Euclidean distance between the centers of those two cells and δ is the distance in units between the centers of two adjacent cells (δ is a function of the width of channel between cells).

Let $Cell_A$, $Cell_B \subset A$ be two cell spaces, we define the directed Hausdorff distance, d_H, by:

$$d_H\left(Cell_A, Cell_B\right) = \max_{C_a \in Cell_A} \min_{C_b \in Cell_B} D\left(C_a, C_b\right) \tag{3.3}$$

Thus $d_H\left(Cell_A, Cell_B\right)$ gives the minimum distance from the cell $C_a \in Cell_A$ to any cell in $Cell_B$, where C_a is the cell in $Cell_A$ furthest from any cell in $Cell_B$. The Hausdorff distance D_H is given by

$$D_H\left(Cell_A, Cell_B\right) = \max\left(d_H\left(Cell_A, Cell_B\right), d_H\left(Cell_B, Cell_A\right)\right) \qquad (3.4)$$

Example in Figure 15, shows how these definitions work. Placing the origin in the bottom left corner of the ambient space, the configuration of cells is:

$$C_a = \{(16,5),(16,16),(16,27),(27,16)\}$$
$$C_b = \{(5,5),(27,27),(38,16),(49,16)\}$$

and in terms of cell space:

$$Cell_A = \{(i,j) \mid i \in \{12,\ldots,20\},\ j \in \{1,\ldots,9,12,\ldots,20,23,\ldots,31\}\} \cup \{(i,j) \mid i \in \{23,\ldots,31\},\ j \in \{12,\ldots,20\}\}$$
$$Cell_B = \{(i,j) \mid i,j \in \{1,\ldots,9\}\} \cup \{(i,j) \mid i,j \in \{23,\ldots,31\}\} \cup \{(i,j) \mid i \in \{34,\ldots,42,45,\ldots,53\},\ j \in \{12,\ldots,20\}\}$$

An easy calculation shows that $d_H(Cell_A, Cell_B) = \sqrt{2}$, $d_H(Cell_B, Cell_A) = 2$ and $D_H(Cell_A, Cell_B) = 2$.

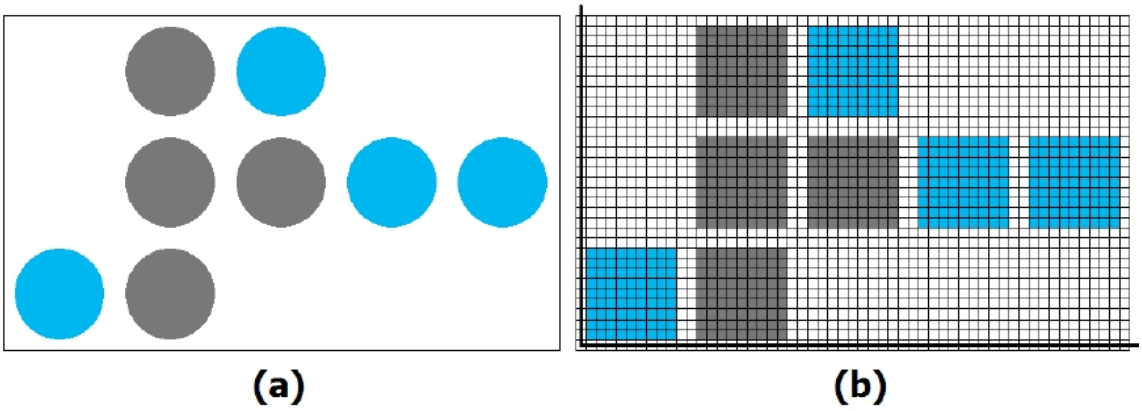

Figure 15 - $Cell_A$ (grey) and $Cell_B$ (light blue) discretized as circles (a) or squares (b, with axes included)

The next definition introduces the notion of walk between two biological cells:

DEFINITION - Let C_a, C_b be two cells. A walk from C_a to C_b is a sequence of cells, $\{C_{a_i}\}_{i=0}^{n}$, such that $C_a = C_{a_0}, C_b = C_{a_n}$ and $D(C_{a_j}, C_{a_{j+1}}) = 1$ for $j = 0,1,\ldots,n-1$.

A walk $\{C_{a_i}\}_{i=0}^{n}$ is minimal if $\max_{j=0,1,\ldots n} \min(D(C_{a_0}, C_{a_j}), D(C_{a_j}, C_{a_n})) \leq \max_{j=0,1,\ldots m} \min(D(C_{b_0}, C_{b_j}), D(C_{b_j}, C_{b_m}))$ for any other walk $\{C_{b_i}\}_{i=0}^{m}$ with $C_a = C_{b_0}, C_b = C_{b_m}$.

Clearly, a walk must "cross" the line equidistant (using the Euclidian metric) to the two end-point cells C_a and C_b. We will call any cell through which this line passes a "middle cell". Notice that for some scenarios, there might not be any middle cell (Figure 16,a). This can be the case only if the first or second indices of the cells C_a and C_b coincide. Assume that C_a and C_b are not aligned, then middle cells exists and it is clear that a minimal walk must contains a middle cell such that the sum of its distance to C_a and its distance to C_b is less or equal to this sum for any other middle cell. It is also true that this distance represents the value $\max_{j=0,1,\ldots n} \min(D(C_{a_0}, C_{a_j}), D(C_{a_j}, C_{a_n}))$.

PROPOSITION - Let C_a, C_b be two cells in the ambient space. Then, there exists a minimal walk from C_a to C_b. The minimal walk may not be unique.

The proof is based on our previous remarks. First let us introduce a specific construction for a walk between $C_a = (i_a, j_a)$ and $C_b = (i_b, j_b)$, we will prove that it is minimal. We introduce

$$d_i = \begin{cases} \left\lfloor \frac{i_b - i_a}{2\delta} \right\rfloor & if \quad i_b - i_a \geq 0 \\ \left\lceil \frac{i_b - i_a}{2\delta} \right\rceil & if \quad i_b - i_a \geq 0 \end{cases}$$

$$d_j = \begin{cases} \left\lfloor \frac{j_b - j_a}{2\delta} \right\rfloor & if \quad j_b - j_a \geq 0 \\ \left\lceil \frac{j_b - j_a}{2\delta} \right\rceil & if \quad j_b - j_a \geq 0 \end{cases}$$

as the as the horizontal and vertical integer part distances. If $d_i \leq 2$ and $d_j \leq 2$, the minimal walk is straightforward to construct. Otherwise, we construct a minimal walk inductively by finding a minimal walk between (i_a, j_a) and $(i_a + d_i, j_a + d_j)$ and a minimal walk between $(i_b - d_i, j_b - d_j)$ and (i_b, j_b), if the horizontal and vertical integer part distances between these two indices are greater than 2 we keep subdividing. We concatenate these minimal walks to achieve a walk between (i_a, j_a) and (i_b, j_b). This final walk is minimal. Indeed, its middle point is the furthest unit in the walk from either C_a or C_b but by construction it is also the closest cell from C_a and C_b among the set of all middle cells (and this is also true for each of the subdivision). □

Notice that it is not true that the concatenation of two minimal walks is always also a minimal walk.

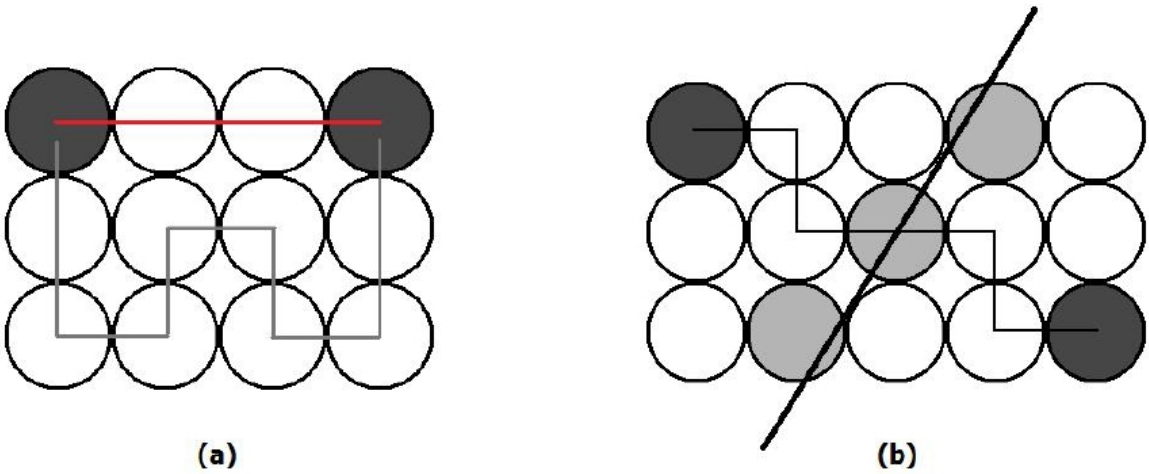

Figure 16 - Walks between cells

(a) Two example walks, one of which is a minimal walk. (b) A minimal walk, with middle cells highlighted. Note that any minimal walk must pass through the middle cell in the center, and will not pass through any other middle cell.

DEFINITION - A cell space $Cell$ is called 1-connected if for any two cells, $C_a, C_b \in Cell$, there exists a walk $\{C_{a_i}\}$ with $C_{a_i} \in Cell$ for all i and $C_{a_0} = C_a, C_{a_n} = C_b$. More generally, $Cell$ is said to be r-connected if there exist a sequence $\{C_{a_i}\}_{i=0}^{n}$ with $C_{a_i} \in Cell$ for all i, $C_{a_0} = C_a, C_{a_n} = C_b$ and such that $D(C_{a_j}, C_{a_{j+1}}) \le r$ for $j = 0,1,\ldots,n-1$. We call $Cell$ minimally r-connected if $Cell$ is r-connected but not m-connected for any $m < r$.

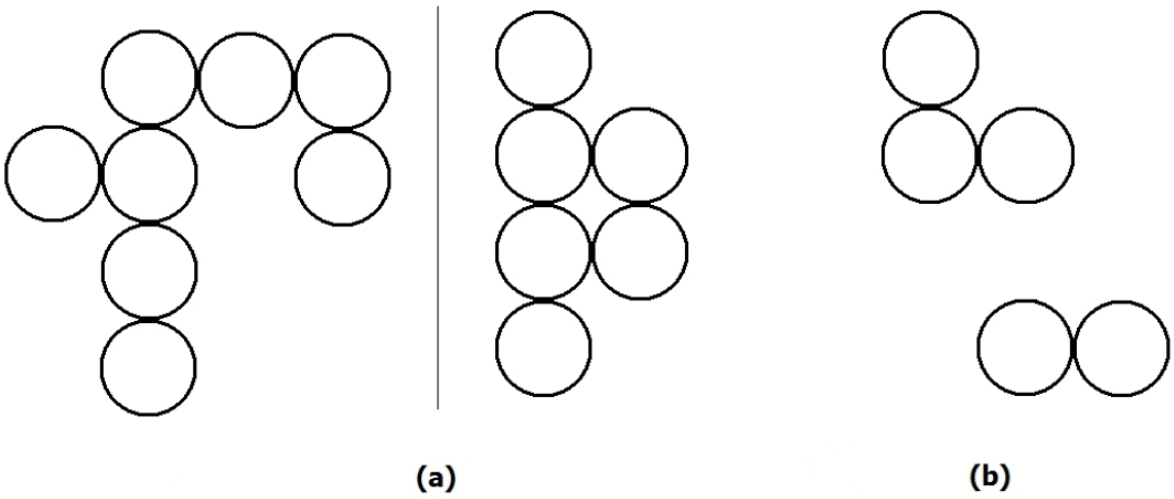

Figure 17 - (a) 1-connected cell space, (b) minimally 3-connecrted cell space

DEFINITION - Let $Cell_A$ and $Cell_B$ be two cell spaces. A path (when it exists) between $Cell_A$ to $Cell_B$ is a sequence of morphogenic events such that $Cell_A$ deforms into $Cell_B$. More precisely, the existence of a path is equivalent to the existence of an initial value X(0) and an admissible control $u(\cdot)$ defined on $[0,T]$, $Cell_A = Cell(0)$ such that there is a solution to problem with $Cell_B = Cell(T)$. Given the fact that in this section we neglect the role of the growth factor, it boils down to the existence of a dynamic spatial distribution of fractones that generates the desired growth.

PROPOSITION - Given an initial cell space $Cell(0)$ and a 1-connected cell space $Cell_F$ such that $Cell(0) \subset Cell_F$, then there exists a path from $Cell(0)$ to $Cell(T)$ for some T such that $D_H(Cell(T), Cell_F) \leq 1$.

Since $Cell(0)$ is assumed to be a strict subset of $Cell(T)$, let $C_{a_0} \in Cell(0)$ such that there exists $C_{a_1} \in Cell(T)$ with $D(C_{a_0}, C_{a_1}) = 1$ and $C_{a_1} \notin Cell(0)$ (i.e. C_{a_1} must be directly above, below, to the right, or to the left of C_{a_0}). This is possible since $Cell(T)$

is 1-connected. We activate a fractone associated to the cell C_{a_0} to induce mitosis. If C_{a_1} is to the right of C_{a_0}, then when growth is triggered, the mass of cell deforms and C_{a_1} is brought into the new cell space. If C_{a_1} is below, to the left, or above C_{a_0}, then growth must occur at least two, three, or four times, respectively, before the mass of cell deforms in the C_{a_1} direction. The extra cells created in this growth will be distance 1 from C_{a_0}, and therefore either in $Cell_F$ or a distance 1 from $Cell_F$. Inductively, we inactivate the fractone and repeat the process. When no cell C_{a_0} satisfying our assumptions exists, then the newly obtained cell space at that time, T, must be within Hausdorff distance 1 since no extra cell created was more than distance 1 from any element of $Cell_F$. □

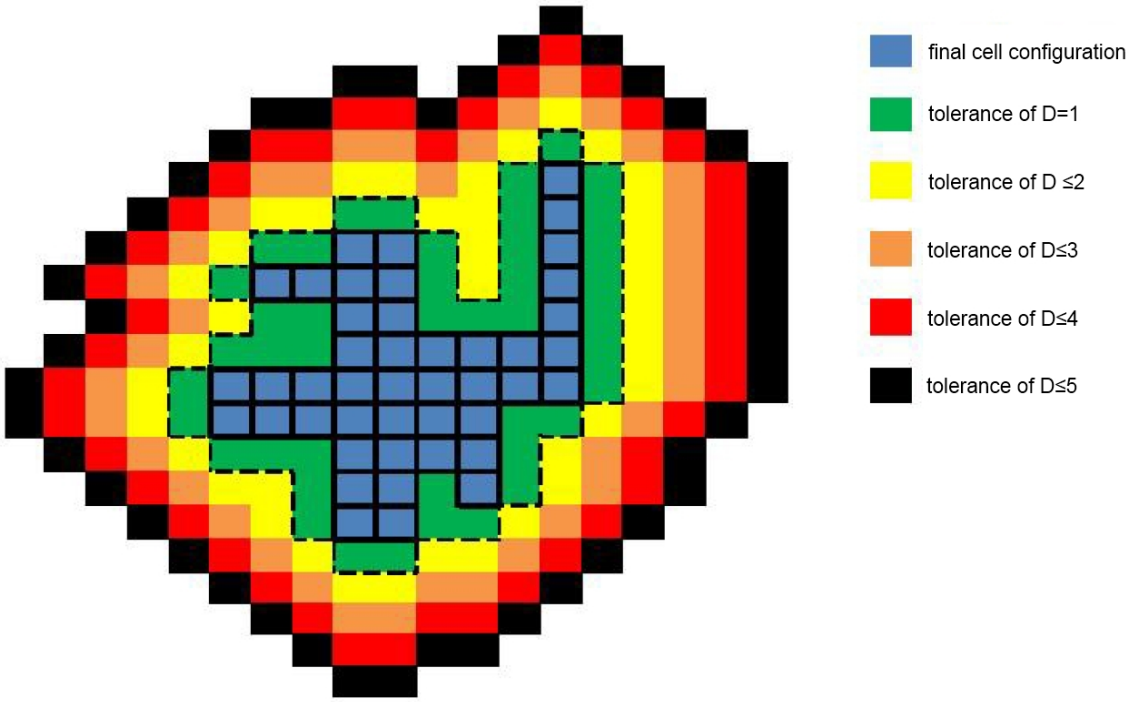

Figure 18 - Distance from a configuration

From any initial cell space included in the final cell space represented in blue can be deformed into a cell space strictly included in the green space at Hausdorff distance 1 of the desired final cell space.

The next natural question is to determine how to modify the deformation algorithm in order to replace the existence of a path from $Cell(0)$ to $Cell(T)$ for some T such

that $D_H(Cell(T), Cell_F) \leq 1$ by the existence of a path such that $Cell(T) = Cell_F$, i.e. we can reach exactly the final prescribed cell space. The following proposition states that we can improve the accuracy of the growth if we allow rotation of the entire configuration space between growth events. This is not surprising since it essentially allows us to choose the direction of cell growth

PROPOSITION - Given an initial cell space $Cell(0)$ and a 1-connected cell space $Cell_F$ such that $Cell(0) \subset Cell_F$, then, with rotations of the configuration space allowed between morphogenic events, there exists a path from $Cell(0)$ to $Cell(T)$ for some T such that $D_H(Cell(T), Cell_F) = 0$.

Let $C_{a_0} \in Cell(0)$ such that there exists $C_{a_1} \in Cell(T)$ with $D(C_{a_0}, C_{a_1}) = 1$ and $C_{a_1} \notin Cell(0)$. Rotate $Cell(0)$ and $Cell_F$ together until C_{a_1} (or its rotational image) lies to the right of C_{a_0} (or its rotational image). We then proceed exactly as in previous proposition by activating a fractone associated to cell C_{a_0}. The cell space is then deformed exactly in the Ca1 direction. Since $Cell_F$ is connected, this process can be repeated, and the cell space rotated back to its original orientation, until $D_H(Cell(T), Cell_F) = 0$. □

One should note this path from $Cell(0)$ to $Cell(T)$ is neither unique nor time-optimal. In fact, it is quite slow as at most 1 fractone is active at any given time. Notice also that from the biological point of view, a deformation algorithm that allows translation and rotation of the cell space is not realistic for several reasons. It is interesting purely from a mathematical point of view.

The next result concerns a cell growth from an initial cell space to reach as close as possible a final cell space that is minimally r-connected, $r > 1$. Let us first state a useful lemma.

LEMMA - Let $C_i = (i_i, j_i),\ i = 1,2$ be two cells in a cell space such that $D(C_1, C_2) = r$, r odd . Then for the middle point $C_m = (i_m, j_m)$ of a minimal walk between C_1 and C_2, $\min\left(D(C_1, C_m), D(C_m, C_2)\right) \le \frac{r}{\sqrt{2}}$.

Let $d_i = \frac{|i_2 - i_1|}{\delta}$ and $d_j = \frac{|j_2 - j_1|}{\delta}$. Then $r = \sqrt{d_i^2 + d_j^2}$. We first note that the case where either d_i or d_j equal 0 is trivial. The minimal walk is a straight row or column, and the distance to a middle cell is equal to $\frac{r}{2}$ (if r is even there is no middle cell). If $d_i = 1$ and $d_j = 1$, then it is simple to verify that $r = \sqrt{2}$ and the distance to the middle points is 1. Otherwise, in general, there are three cases: (i) d_i, d_j both even; (ii) one of d_i, d_j odd; (iii) or both d_i, d_j odd.

Case (i): If d_i, d_j both even, then the middle point is a distance $\sqrt{\left(\frac{d_i}{2}\right)^2 + \left(\frac{d_j}{2}\right)^2} = \frac{r}{2} < \frac{r}{\sqrt{2}}$ from either C_1 or C_2.

Case (ii): Without loss of generality, suppose d_i is odd and d_j is even. Then the furthest distance from the middle point of a minimal walk to either C_1 or C_2 will be $\sqrt{\left(\frac{d_i + 1}{2}\right)^2 + \left(\frac{d_j}{2}\right)^2} = \frac{1}{2}\sqrt{d_i^2 + d_j^2 + 2d_i + 1} \le \frac{1}{\sqrt{2}}\sqrt{d_i^2 + d_j^2}$ if $2d_i + 1 \le d_i^2 + d_j^2$. Since $d_i \ge 2$ and $d_j \ge 1$ (otherwise we would be in one of the previously proven cases), the inequality holds.

Case (iii): If both d_i, d_j are odd (note in this case $d_i \ge 3$ and $d_j \ge 3$), then the furthest distance from the middle point of a minimal walk to either C_1 or C_2 is $\sqrt{\left(\frac{d_i + 1}{2}\right)^2 + \left(\frac{d_j + 1}{2}\right)^2}$. It follows that $\sqrt{\left(\frac{d_i + 1}{2}\right)^2 + \left(\frac{d_j + 1}{2}\right)^2} \le \frac{1}{\sqrt{2}}\sqrt{d_i^2 + d_j^2}$ if $2d_i - 2d_j + 2 \le d_i^2 + d_j^2$. Since $d_i \ge 3$ and $d_j \ge 3$, the inequality holds (the same

argument is true if we invert i and j in the equations depending on the minimal walk that has been chosen). □

PROPOSITION - Given an initial cell space $Cell(0)$ and a minimally r-connected cell space, $r>1$, $Cell_F = \bigcup_{i=1}^{n} Cell_{F_i}$ where each $Cell_{F_i}$ is 1-connected. Assume $Cell(0) \subset Cell_{F_k}$ for some k. Then there exists a path from $Cell(0)$ to $Cell(T)$ for some T such that $D_H(Cell(T), Cell_F) \le \frac{r}{\sqrt{2}}$

First, we construct from $Cell_F$ a new cell space by bridging the gaps between all its components $Cell_{F_i}$. The algorithm goes as follows: find the cell in $Cell_{F_1}$ and the cell in $\bigcup_{i\neq 1} Cell_{F_i}$ that have minimal distance D to each other. Find a minimal walk between these two cells, call it $\{C_{a_{1i}}\}$. Without loss of generality, suppose we connect $Cell_{F_1}$ and $Cell_{F_2}$. Then find a cell in $Cell_{F_1} \cup Cell_{F_2}$ and a cell in $\bigcup_{i>2} Cell_{F_i}$ that minimize the distance D between all cells in those two cell spaces. Again, find a minimal walk between these two cells, call it $\{C_{a_{2i}}\}$. Proceed

iteratively until all $Cell_{F_i}$ have walks, $\{C_{a_{ji}}\}$, between them. Then let $Cell_G$ be the union of $Cell_F$ and $\bigcup_{j=1}^{n-1} \{C_{a_{ji}}\}$. Then $Cell_G$ is 1-connected, so by previous proposition, there exists a path from $Cell(0)$ to $Cell(T)$ for some T such that $D_H(Cell(T), Cell_G) \le 1$. The difference between $Cell_F$ and $Cell_G$ are the minimal walks, so the Hausdorff distance from $Cell(T)$ to $Cell_F$ will be at most the maximum distance from a walk endpoint to a point $\sqrt{2}$ away from the closest middle cell. Since $Cell_F$ is minimally r-connected, we need only to consider the walks between cells at a distance r from each other. Let $C_i = (i_i, j_i),\ i = 1,2$ be two such cells, and let $d_i = \frac{|i_2 - i_1|}{\delta}$ and $d_j = \frac{|j_2 - j_1|}{\delta}$. Then $r = \sqrt{d_i^2 + d_j^2}$. Suppose first that d_i is 0. We note d_j cannot be equal one since we

assume $Cell_F$ is not 1-connected. If $d_j \geq 3$ is odd, then the minimal walk between C_1 and C_2 is a column of cells, and the minimum of the maximum distances to a cell one away (left or right) from this walk is given by $\sqrt{\left(\frac{d_j - 1}{2}\right)^2 + 1}$. This will be less than or equal to $\frac{r}{\sqrt{2}}$ if $d_j^2 + 2d_j \geq 5$, which is true for $d_j \geq 3$. Similarly, if $d_j \geq 2$ is even, then the distance to a cell one away from the middle cell is: $\sqrt{\left(\frac{d_j}{2}\right)^2 + 1}$. Note that $\sqrt{\left(\frac{d_j}{2}\right)^2 + 1} \leq \frac{r}{\sqrt{2}}$ if $d_j^2 \geq 4$, which is always true for $d_j \geq 2$. Remark that the above argument applies even if the values of d_i and d_j are swapped (covering the case where the minimal walk is a horizontal row of cells), and covers the worst-case scenario; clearly, growing to the right along a horizontal minimal walk will match the minimal walk exactly, giving a Hausdorff distance within $r/2$, while growing to the left requires to pass through a middle cell above or below the middle cell of the minimal walk. Suppose now that neither d_i nor d_j are 0. If both d_i and d_j are even, then the minimal walk must pass through the middle cell $C_{M_1} = (i_1 \pm d_i/2, j_1 \pm d_j/2)$, where the $\pm$ is determined by the relative position of C_1 to C_2. Then the maximum distance from an end cell of the walk (i.e. C_1, C_2) to a cell within $\sqrt{2}$ of C_{M_1} is $\sqrt{\left(\frac{d_i}{2}+1\right)^2 + \left(\frac{d_j}{2}-1\right)^2}$ (or equivalently we can interchange i and j). Moreover, $\sqrt{\left(\frac{d_i}{2}+1\right)^2 + \left(\frac{d_j}{2}-1\right)^2} \leq \frac{r}{\sqrt{2}}$ if $(d_i^2 - 4d_i) + (d_j^2 + 4d_j) \geq 8$, which is always true for $d_i, d_j \geq 2$. The case of $d_i = d_j = 1$ is trivial. So suppose d_i and d_j are both odd and not both 1. Then there are two middle cells the minimal walk could pass through. Without loss of generality, let it pass through $\left(i_1 + \frac{d_i + 1}{2}, j_1 + \frac{d_j - 1}{2}\right)$. Then the neighboring cells of interest are

$C_{N_1} = \left(i_1 + \frac{d_i - 1}{2}, j_1 + \frac{d_j + 1}{2} \right)$ and $C_{N_2} = \left(i_1 + \frac{d_i + 3}{2}, j_1 + \frac{d_j - 3}{2} \right)$. The distance from C_1 to C_{N_1} is $\sqrt{\left(\frac{d_i + 1}{2} \right)^2 + \left(\frac{d_j - 1}{2} \right)^2}$. And this is less than $\frac{r}{\sqrt{2}}$ if $(d_i^2 - 2d_i) + (d_j^2 + 2d_j) \geq 2,$ which is always true for $d_i, d_j \geq 1$. The distance from C_1 to C_{N_2} is $\sqrt{\left(\frac{d_i + 3}{2} \right)^2 + \left(\frac{d_j - 3}{2} \right)^2}$. And this is less than $\frac{r}{\sqrt{2}}$ if $(d_i^2 - 6d_i) + (d_j^2 + 6d_j) \geq 18,$ which is always true for $d_i, d_j \geq 3$. It fails in the cases when $d_i \leq 7$ and $d_j = 1$, however in these cases, it turns out that C_{N_2} is closer to C_2 than to C_1 and it is easy to show that a walk can still be grown that satisfies the desired conclusion (see Figure 19). Finally suppose now, without loss of generality, that d_i is odd and d_j is even. Assume that one of the middle cells of the minimal walk is $C_{M_2} = (i_1 + (d_i - 1)/2, j_1 + d_j/2)$ (other cases are similar). By symmetry, a second middle cell that the minimal walk must pass through is $C_{M_3} = (i_1 + (d_i + 1)/2, j_1 + d_j/2)$. C_{M_2} is closer to C_1 than to C_2, and similarly, C_{M_3} is closer to C_2 than to C_1. Therefore, in calculating Hausdorff distance, we need only look at the distances between cells neighboring C_{M_2} and C_1. By symmetry, these will be the same as the distances between points neighboring C_{M_3} and C_2. The neighboring cells to C_{M_2} are $C_{N_3} = (i_1 + (d_i - 3)/2, j_1 + (d_j + 2)/2)$ and $C_{N_4} = (i_1 + (d_i + 1)/2, j_1 + (d_j - 2)/2)$. The distance to C_{N_3} is $\sqrt{\left(\frac{d_i - 3}{2} \right)^2 + \left(\frac{d_j + 2}{2} \right)^2}$, less than or equal to $\frac{r}{\sqrt{2}}$ if $(d_i^2 + 6d_i) + (d_j^2 - 4d_j) \geq 13,$ which holds except in the cases where $d_i = 1$ and $d_j \leq 4$. However, as in the previous case, it is easy to show that a walk can still be grown that satisfies the desired conclusion. The distance to C_{N_4} is

$\sqrt{\left(\frac{d_i+1}{2}\right)^2+\left(\frac{d_j-2}{2}\right)^2}$, less than or equal to $\frac{r}{\sqrt{2}}$ if $(d_i^2-2d_i)+(d_j^2+4d_j)\geq 5$, which holds for $d_i \geq 1$ and $d_j \geq 2$. □

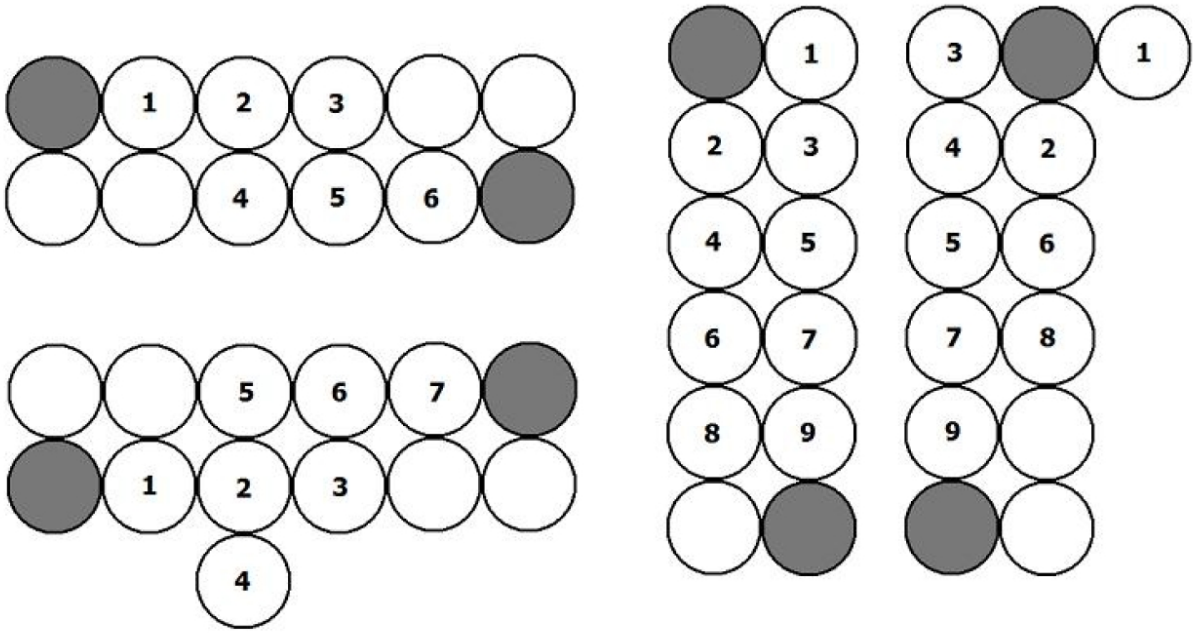

Figure 19 - Possible configuration at same Hausdorff distance

The four possible configurations when $d_i = 1$, $d_j = 5$ or $d_i = 5$, $d_j = 1$. Cells are numbered by order of growth.

The Hausdorff distance in all four cases is $\sqrt{5}$

PROPOSITION - Given an initial cell space $Cell(0)$ and a minimally r-connected cell space, $Cell_F = \bigcup_{i=1}^{n} Cell_{F_i}$ where each $Cell_{F_i}$ is 1-connected. Assume $Cell(0) \subset Cell_{F_k}$ for some k. Then, with rotations allowed between morphogenic events, there exists a path from $Cell(0)$ to $Cell(T)$ for some T such that $D_H(Cell(T), Cell_F) \leq \frac{r}{\sqrt{2}}$

As in the above proof, we construct a new cell space, $Cell_G$, that bridges the gaps between each $Cell_{F_i}$. We showed already that there exists a path from $Cell(0)$ to

$Cell(T)$ such that $D_H(Cell(T), Cell_G) = 0$. $Cell_F$ differs from $Cell_G$ solely by the minimal walks. Thus $D_H(Cell_G, Cell_F)$ is the distance from the cell on a minimal walk which is furthest from any point in $Cell_F$. This must be one of the middle cells of a minimal walk. Since $Cell_F$ is minimally r-connected, the longest minimal walk(s) must connect cells a distance r apart. Therefore, thanks to the lemma introduced above, $D_H(Cell_G, Cell_F) \leq \frac{r}{\sqrt{2}}$. □

In this section, we presented some answers to the one of the most basic question, which is the existence of a path between two given cell spaces. Clearly, much is still to be answered. One strategy to be explored in forthcoming work is based on the experimental observations collected in the lab through the fractone maps. Indeed, the experimental maps will provide information about the control function used by nature to produce morphogenic events. Based on those observations as well as assumptions such as minimizing the number of times mitosis can take place during the entire duration of the morphogenic event or minimizing the number of switching in the control function (which is equivalent to minimize the changes in the spatial distribution of the fractones), we can ascribe a cost function to be minimized. Our problem then becomes an optimal control problem. The bottom line is that, due to the complexity of the system, there is an extremely large number of questions associated to this problem, and, as said previously, new methods need to be developed.

Our model clearly diverges from Turing's model (or any other Reaction-Diffusion model), and it presents new challenges that will advance the field of control theory. To envision how our problem does this, we must compare and contrast versus typical control theory problems. For example, in physics, the state space is static and the equations of motion are derived from minimizing a Lagrangian. In engineering, the configuration manifold is fixed and one either attempts to determine the evolution of the system while minimizing a prescribed cost or one tries to design controls to take into account uncertainties of the system. Due to the morphogenic nature of the biological process under study, the configuration space is constantly evolving (caused by the

creation of new cells), and thus cannot be analyzed using traditional techniques of control theory in which the equations describing a given system are predetermined when defining the system. This distinguishes in a very non-trivial way our problem from the traditional problems whose systems are usually defined on a static configuration space.

Inspired by the biological question, we propose an entirely new theoretical control problem by noting that an intrinsic property of biological systems is having a dynamic state space. As a result, new methods have to be proposed to analyze these type of systems from the control theory point of view. This will advance the field of control theory by considering new problems and by providing insight toward the development of innovative ideas and methods to solve these types of problems.

4. MODEL IMPROVEMENTS TO FIT BIOLOGICAL EXPERIMENTS

Using computer simulations, by mimicking the assumed system behavior, the model helps us to understand the nonlinear dynamics of the biological system under study. Such approach is especially well suited for biological systems whose complexity renders a purely analytical approach unrealistic. Moreover, it allows us to overcome the excessively demanding purely experimental approach to understand a biological system. At the same time we have to keep always in mind that the study of this particular biological system is not completely accomplished. It is then crucial to work in team with biologists and update our model restating biological issues into a mathematical language. As a result of these considerations we developed a computer model that can be improved relatively easily (although it is quite a complex model) to fit new biological experiments and remarks.

Next sections will show some prior changes to the initial model.

4.1 Growth factor diffusion speed

A first result from computer simulations that does not match with biological evidence is that while the diffusion of growth factors is correctly model in a free ambient space, it results too slow in between cells. We took in account mainly three options to solve this problem:

a) Insert a penalty function for diffusion in the channels between cells
b) Modify the diffusion law from a four-ways to eight-ways direction
c) Increase channel dimension

Defining a penalty function when diffusion occurs in the channel between cells (a) may result in a drastic simplification, as there is no biological evidence that allow us to

properly define such function. Moreover it may lead to loose contact with the biological problem, giving too much arbitrariness to a model that is already wide and complex.

Comparing two simulations with a diffusion of 4 and 8 ways one may think that it is a good option to solve this issue. Unfortunately, option (b) cannot be a good solution from a biological point of view as an eight-ways diffusion process is not reflecting the behavior of the natural process.

In chapter 2 we made the assumption that two adjoining cells are at distance 1 in units (that is d=9 from the centers) and this distance is parameterized by $\delta = 10$. It is then straightforward to relax this assumption changing the value of that parameter, increasing it of one unit: $\delta = 11$. Such modification will not affect the morphogenesis algorithm nor the notion of distance between cells (D) or configurations (D_H).

Although a wider channel between cells does not affect the mitosis process, it has a great effect on the control of our mathematical model: the fractones. We modeled a fractone as a single unit that can be associated up to four cells, but considering a 2-unit channel this assumption has to be modified. We get two options: increase fractones dimension (one may suggest a 2 by 2 square in order not to affect assumptions made in chapter 3) or leave the fractones of the smallest dimension allowed by the mapping and rethink their role in morphogenesis.

Thanks to biological experiments, we decided for the second option. This choice has the immediate result to allow the control to give the input for morphogenesis at only one cell per time, but at the same time, if we aim to have multiple duplications we just need to activate several fractones. Note that for the assumptions made in chapter 2, the definition of time is arbitrary as we modeled mitosis to occur instantaneously.

From this point on, we will consider a 2-unit channel between cells. Thus, we assume that the space between cells accounts for 33% of the total space occupied by the cell.

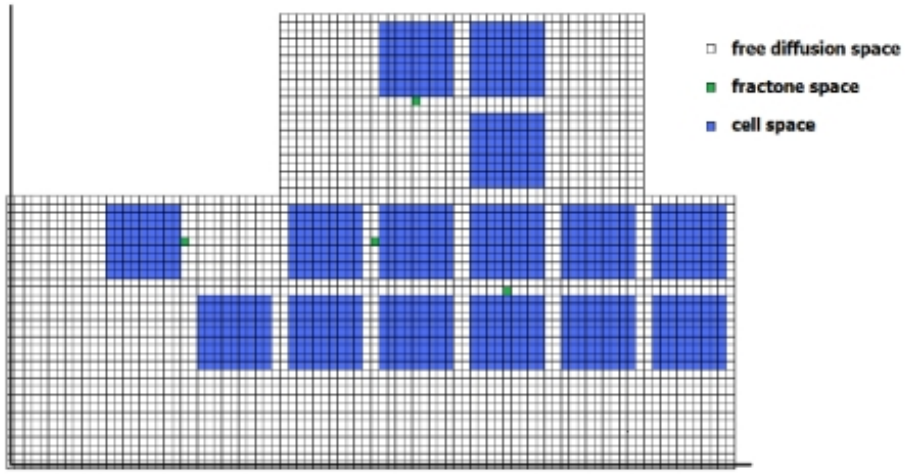

Figure 20 - 2-unit channel between adjoining cells

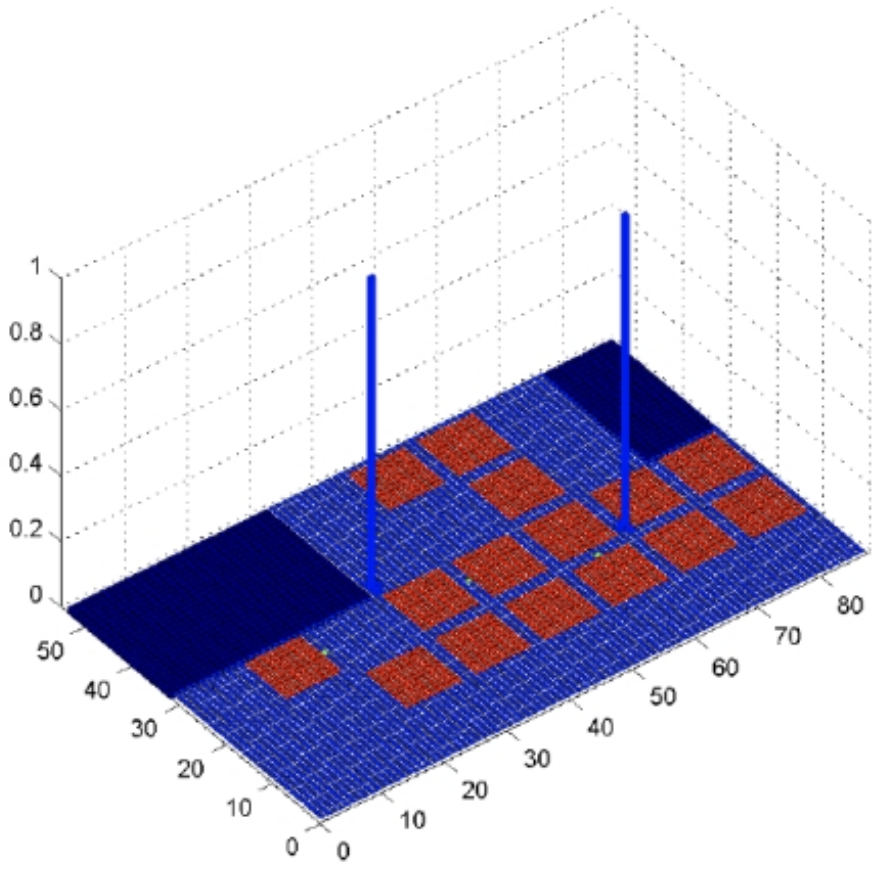

Figure 21 - 2-unit channel between adjoining cells, three dimensional simulation

4.2 Growth factor redistribution

We already modeled how growth factors are redistributed when a new cell is born, but as mitosis is a key element of our model we need to depict this biological process with great attention.

A morphogenic event is described, in biology, by a "mother" cell splitting into two "children". This action perturbs the ambient space as the mass of cells, and growth factors around it, is *pushed* to change its shape and create the exact free space needed for one more cell. Comparing our model with this brutal, but effective, simplification of mitosis, we highlighted two main remarks:

a) As a cell splits into two younger cells, fractones that were around it will be pushed, like a pressure wave, but right after mitosis occurred the channel between the two cells will be empty.
b) In our model we place a new cell at the minimum distance (D) possible instead of rearranging all the existing cells, placing the new cell right next to the mother cell.

Due to the complexity of morphogenesis, scientists cannot define a law that describes how the mass of cells is rearranged yet. Thus we decided to define an algorithm that correctly depicts the arrangement of cells without taking into account the way their absolute position changes, instead of introducing bigger uncertainties through an arbitrary choice. Assumption (b) may be relaxed straightforwardly as soon as an accurate law is found.

We take into account issue (a) by modifying the pressure wave described in (2.9) as follows:

1) we get two options as the new cell $C = (c, d)$:
   I. is on one of the axes superimposed on the "mother" cell (i.e. at $D = 1$)
   II. otherwise (i.e. at $D = \sqrt{2}$)
2) the algorithm calculates the sum of the GF present in the space associated to a cell centered in unit $C = (c, d)$ plus the channel that has to be free of growth factors. See Figure 22 for both I and II cases, respectively.

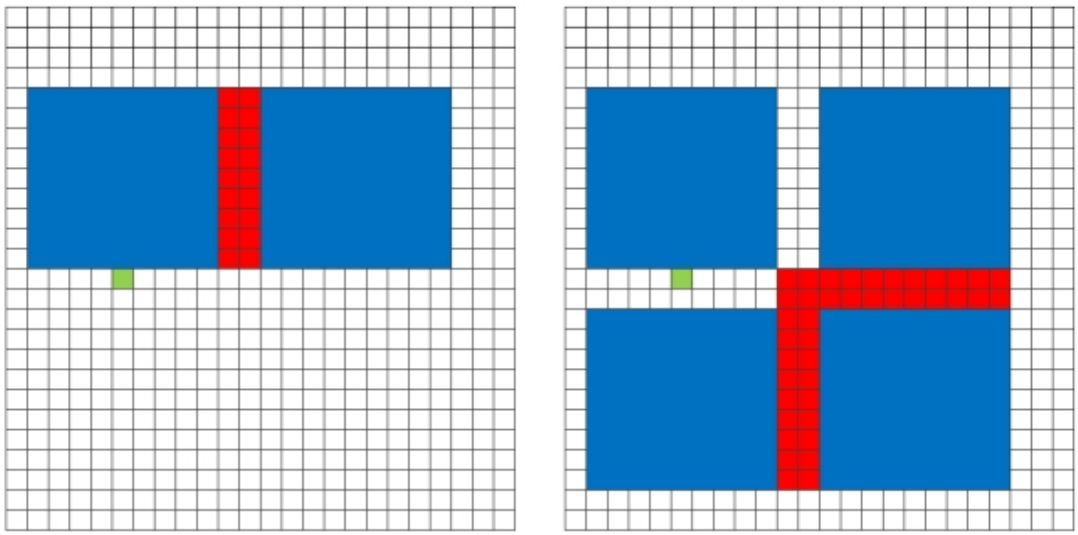

Figure 22 - Channel free from GF after mitosis (in red)

3) deforms $Cell(t)$ such that $(c,d) \in Cell(t)$.

4) counts the number of units in $Free(t) \cup Fract(t)$ that are at a distance $d \leq 8$ from (c,d), excluding the channel defined in (2)
5) distributes 70% of the sum from (1) evenly in each unit from (4).
6) counts the number of units in $Free(t) \cup Fract(t)$ at a distance $8 \leq d \leq 11$ from (c,d), excluding the channel defined in (2)
7) distributes the remaining 30% of the sum from (1) evenly in each unit from (6).

In this way, one can see that once the new cell enters the system, the deformation of $Cell(t)$ creates a "*pressure wave*" that distributes the GF around the space where the deformation impacts $Free(t) \cup Fract(t)$. It should be noted that the distances and percentages chosen are arbitrary and are easily adjustable. In Figure 23, we represent a simulation of a sequence of morphogenic events. We display the cell's duplications as well as the diffusion of growth factors. Accordingly, the GF threshold for a fractone is currently set at 0.4. Notice that we highlighted the cell undergoing mitosis (the "mother" cell) by a green unit in its center.

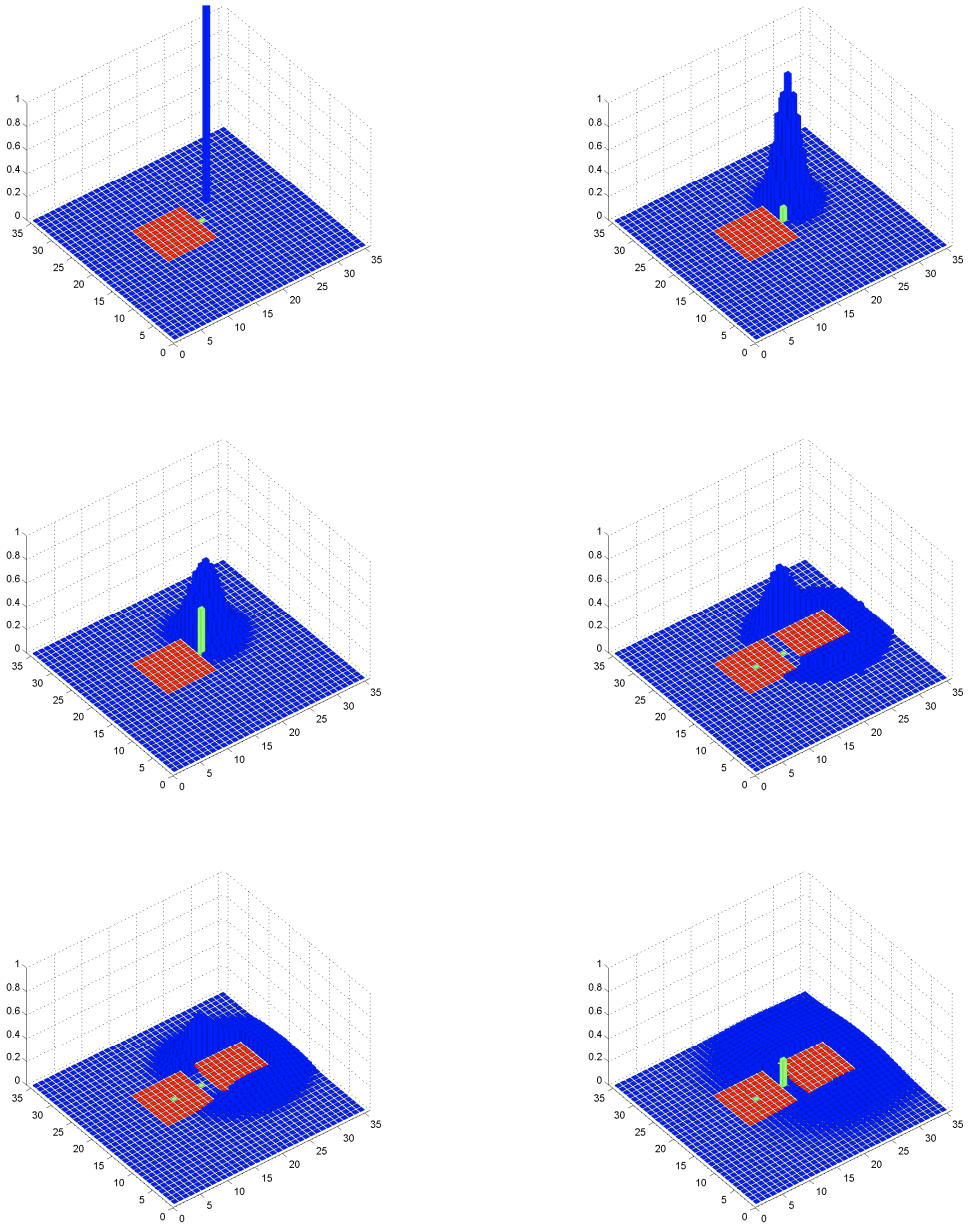

Figure 23 - Growth factor redistridution as a pressure wave

4.3 Growth factor production

Experimental maps show that cells produce growth factor during their entire life. The process of growth factor production seems to be bound up with the age of the cells, that is each cell produces growth factor at a constant rate.

The biological process is defined as a production in the core of the cell and a slow radial diffusion towards the outside. Now recall that we modeled a cell as a space disjoined from $Free(t) \cup Fract(t)$, or rather we can see the boundaries of the cell as walls that prevent diffusion. It comes then natural to embody growth factor production as an instantaneously genesis on the growth factor right outside the cell, with no loss of generality.

The algorithm is extremely simple:

1) As mentioned before, we associate to each cell an age. This depends on the time in which the cell is born.
2) Each cell produces the same amount of growth factor after a fixed interval (Δt)
3) Growth factor is evenly distributed between the neighboring units of the cell (at distance $d = 1$, in units) belonging to $Free(t) \cup Fract(t)$, this is usually 40 units.

These assumptions can be easily relaxed. Table 3 lists the choices adopted for forthcoming simulations (Figure 24).

Time elapsing between subsequent production by the same cell	$\Delta t = 10$
Amount of GF produced	0.1 per unit 3.6 per cell
Distance from the cell borders	$d = 1$

Table 3 - Parameters for GF production

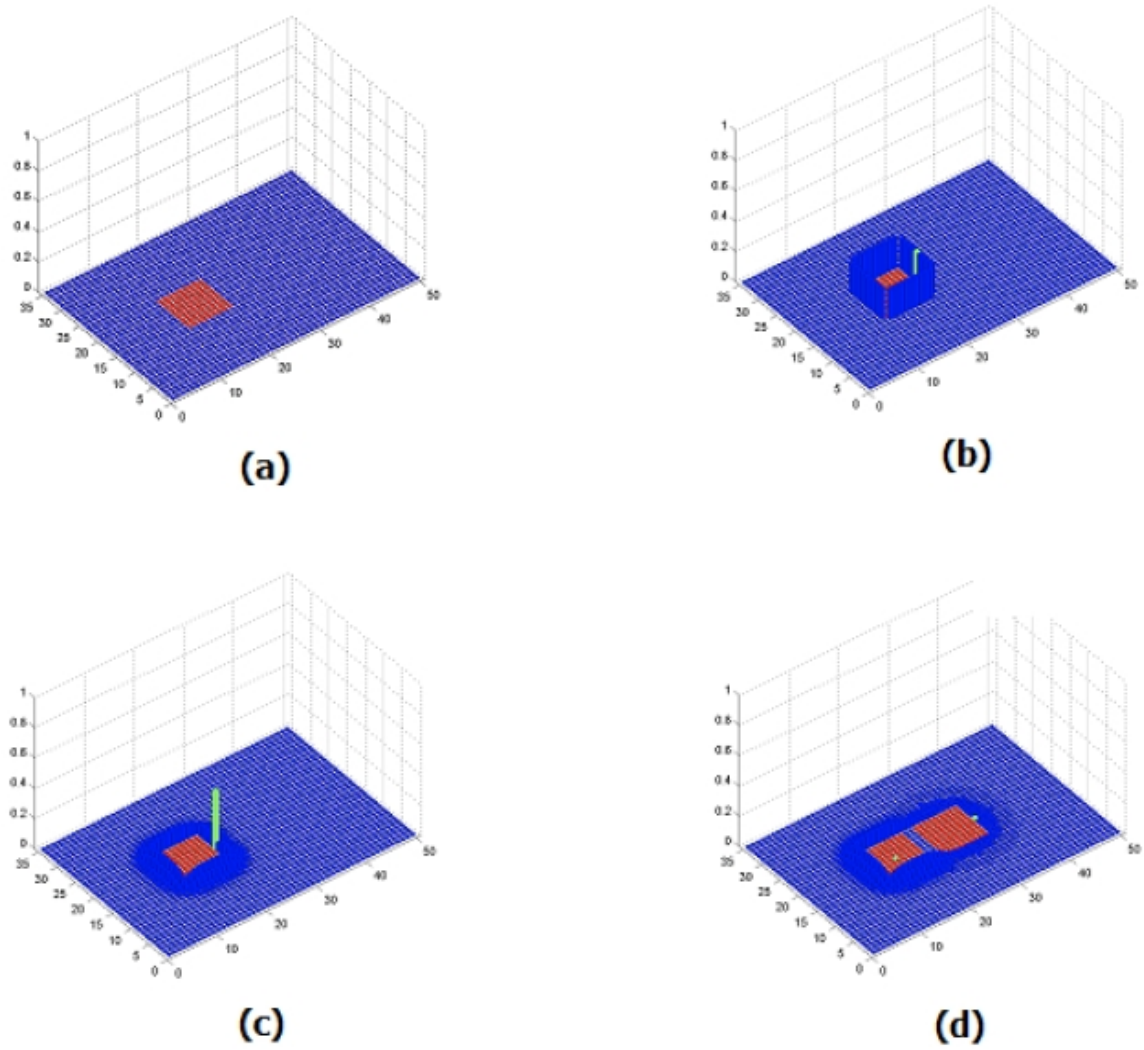

Figure 24 - growth factor production

Note that assumption (2) may be changed, as duplications may be considered the trigger event. In other words, after a certain number of duplications a cell will produce growth factor. By doing so, the algorithm will privilege those cells that replicates more frequently presuming that the control will pick the same cell between the others.

4.4 Fractone activation

Fractones are the control input of our system, described by (2.4), as they capture growth factors and once the stored quantity reaches a given threshold, the fractone

signals to the cells that mitosis can occur. Moreover, a key element in our hypothesis is that the spatial distribution of fractones varies through the sequence of morphogenic events. The role of the function $u(\cdot)$ is precisely to control the location and activation of the fractones.

Recall that the amount of growth factor in an active fractone becomes invisible to the diffusion process, consequently a question arise: what happens to growth factor in unit (i, j), when the control is changed for that unit ($u_{(i,j)} = 0 \to 1$ or $u_{(i,j)} = 1 \to 0$)?

Based on experimental results, when in unit (i, j) occurs a change in the control the algorithm will move the amount of growth factor stored in that unit from $Free(t)$ to $Fract(t)$ and vice versa (Figure 25, where growth factor is evenly distributed in the free space at t=0). Thank to the definition of subspaces, the activation/deactivation of a fractone has no consequence on the structure of the equations ruling the system.

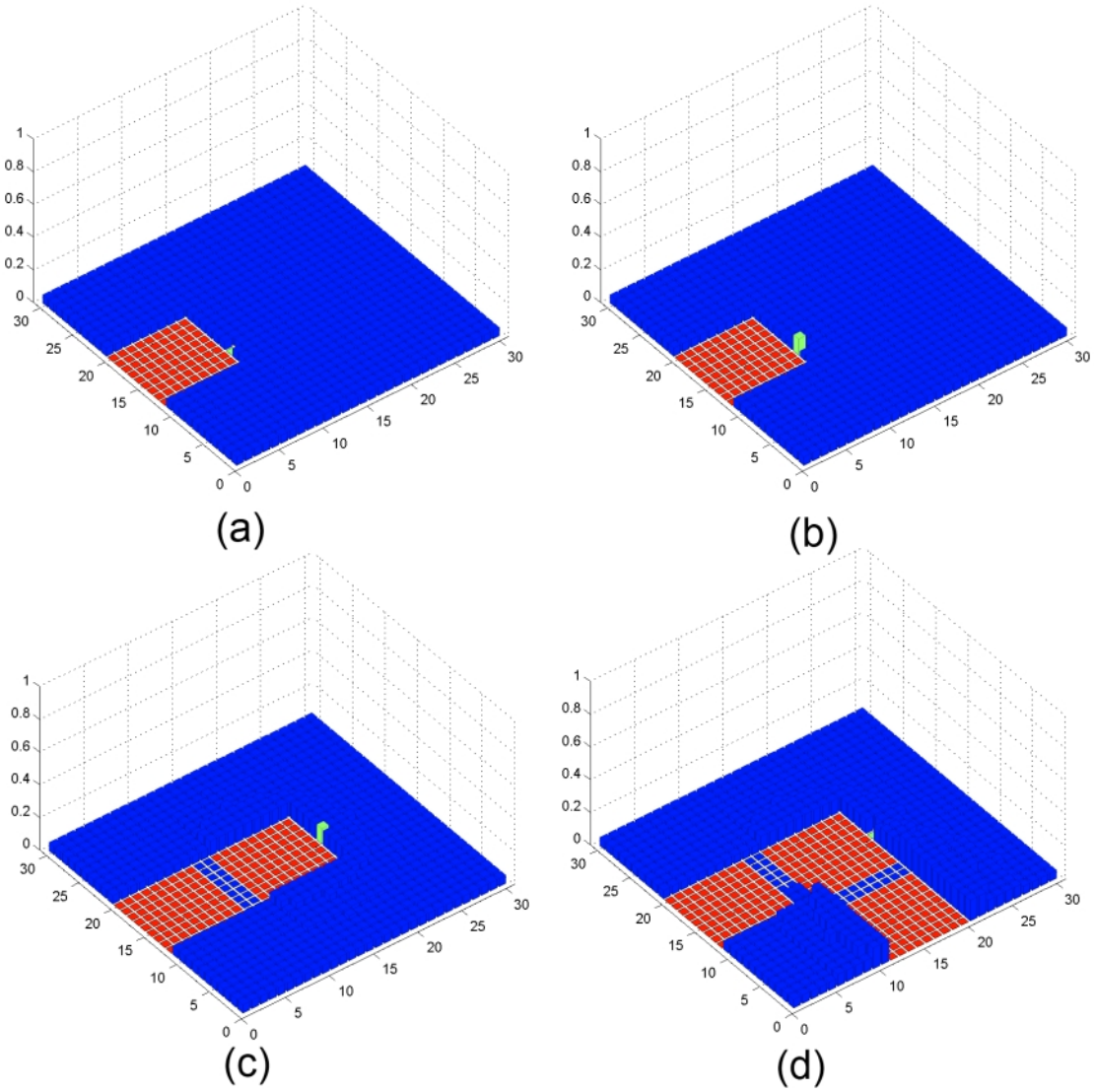

Figure 25 - Fractone activation/deactivation

While defining fractones (and the consequent space associated to them) we made the only assumption that $Fract(t) \subseteq Diff(t)$ (only theoretically, because we will always have $Fract(t) \subset Diff(t)$ and $Free(t) \neq \varnothing$) and this means that a fractone may be active without being associated to a cell. In such configurations the fractone keeps storing growth factor over the set threshold and dictates mitosis as soon as a new cell is formed close enough to it. It is clear that several duplications may occur if the fractone stored an amount of growth factor that is a multiple of the threshold. (Figure 26)

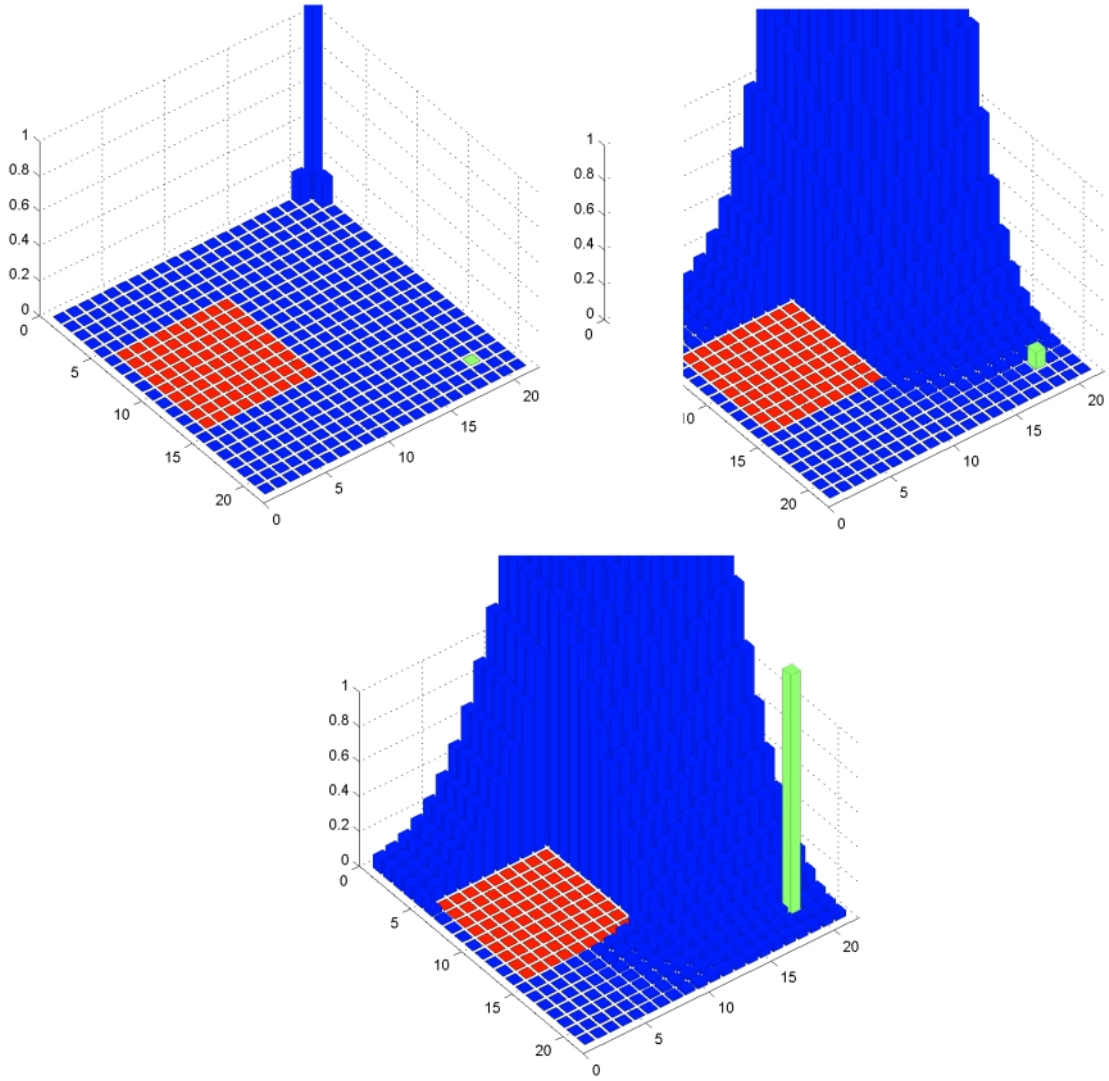

Figure 26 - Fractone not associated to a cell

Notice that a fractone that is not associated to any cell subtracts a unit to $Free(t)$ and this may result in an obstacle in the mitosis process, see Figure 27.

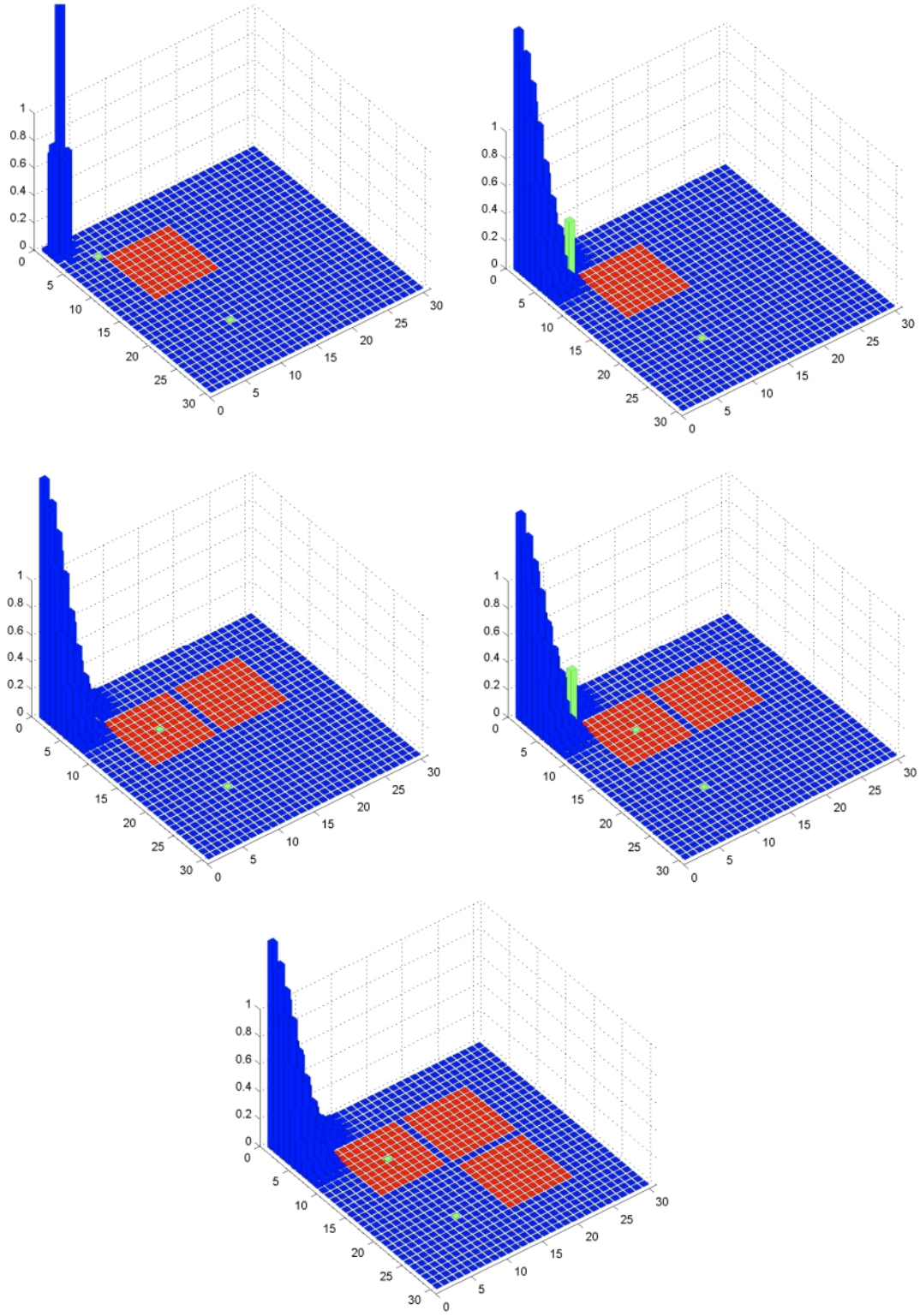

Figure 27 - A fractone resulting in an obstacle

We may now provide an exhaustive simulation, recalling the most crucial rules of our genetic algorithm such as the mitosis algorithm and fractone activation/deactivation in order to control the morphogenic event and reach the desired final configuration.

In Figure 28 we show how it is possible to fill up the ambient space with cells, avoiding obstacles (in black) and using several fractones at each time. Note that we will skip the simulation (with […]) when there is no change in the control for a long time. In order to understand at a glance which cell is undergoing mitosis, that cell is colored in red.

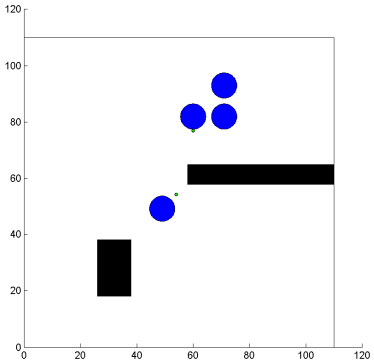
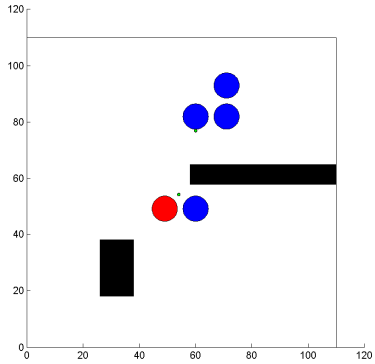
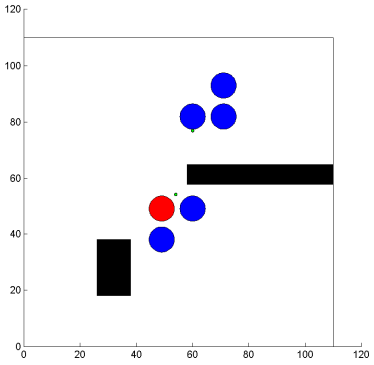
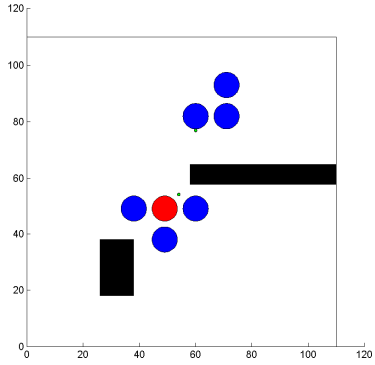
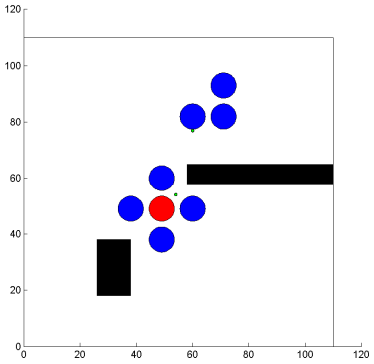
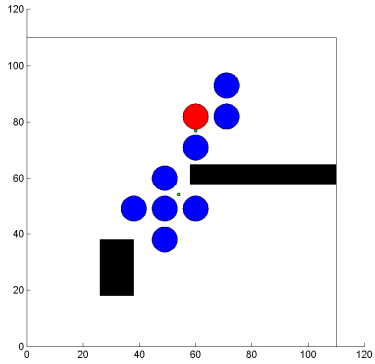
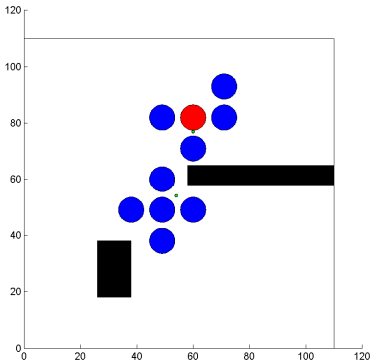
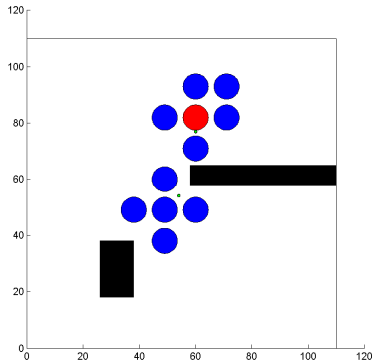

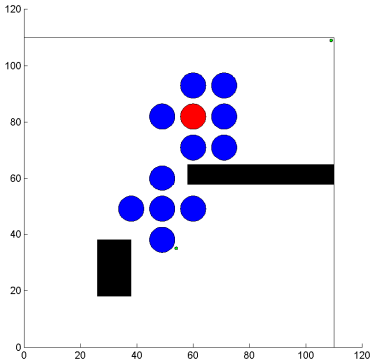
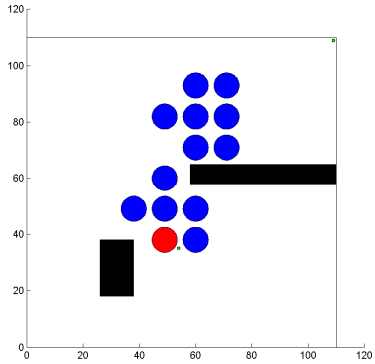
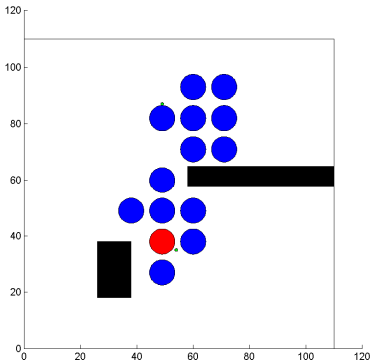
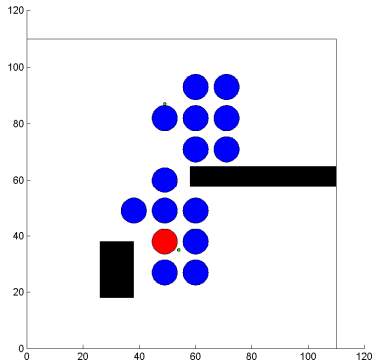
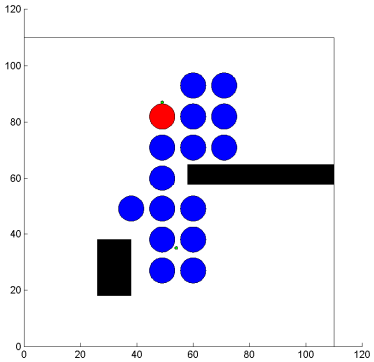

[…]

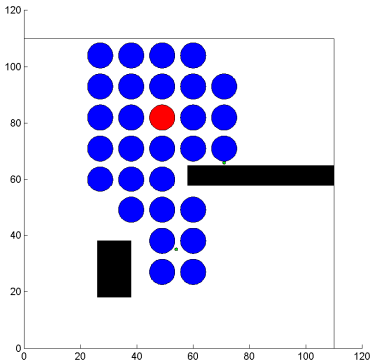
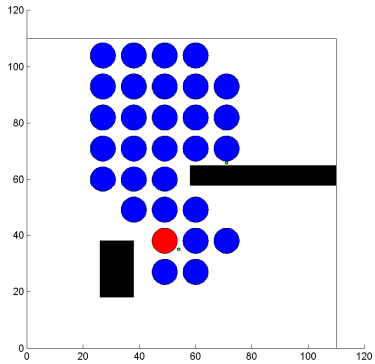

[…]

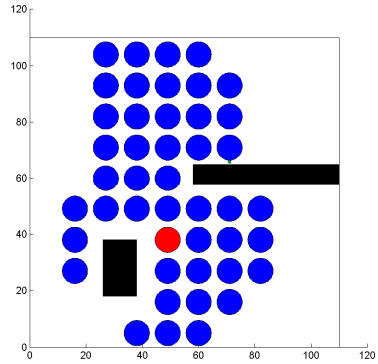

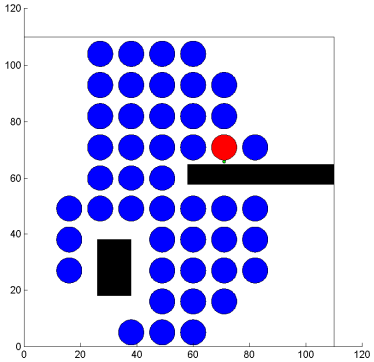

[…]

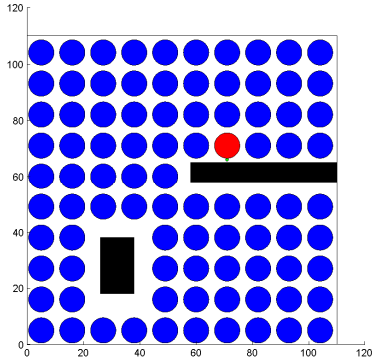

Figure 28 - An exhaustive simulation

5. MATLAB CODE EXPLANATION

The proposed model has been developed under MATLAB®. MATLAB (MATrix LABoratory) is a numerical computing environment developed by MathWorks, MATLAB allows amongst other things: matrix manipulations, plotting of functions and data, implementation of algorithms, creation of user interfaces, and interfacing with programs written in other languages, including C, C++, Java, and Fortran. For this reasons, plus the power in computer calculation, we decided to use this program.

In order to illustrate the code clearly, we will explain the routines combined in categories as they pertain to the same group or they are called after the same trigger event.

5.1 Ambient, variables and subspaces definition

Intuitively, we start our simulation launching *DEFINE_SPACE.M* and the program prompts the user to insert: space dimensions (rectangular ambient space: maxX by maxY), holes position and dimension (in order to modify the ambient space shape), initial configuration of cells and fractones, GF distribution, fractone threshold to give input to mitosis.

The user has to input at least one cell in a valid ambient space: several checks are done in order to avoid border crossing, cells overlapping and creating a fractone inside a cell or an hole, for instance. If no fractones are part of the ambient space for t=0, the code will allow the activation of fractone further on. Equally, if there is no GF at the initial time, cells will produce GF during their life and this will lead to storage by the fractones.

After running *DEFINE_SPACE.M* , the system will be defined by a matrix of maxX rows and maxY colums storing cells position, GF, holes and GF captured by fractones.

5.2 System dynamics

At this stage we run *DYN.M* , starting the simulation. Mathematically, we stated the problem as an ordinary differential equation (ode); thus we used the built-in ode solver ode45, that is a typical solution for a model like this with no stiffness or accuracy problems. The ode solver is called by *SYS_DYNAMICS.M* , and is interrupted if mitosis occurs by *THRESHOLD.M* .

While the simulation is running we may have GF production or fractone activation, both with consequent check if any fractone reached the given threshold. If a fractone reaches the set threshold, this will give the input for mitosis only if said fractone is associated to a cell. The check is made by *FRACT_WITH_CELL.M* .

5.3 Mitosis

When a morphogenic event takes place, the ode solver is interrupted and the system runs *MITOSIS.M* .

At this stage the code looks for the closest set of available cell position (*FREECELL.M*) and if multiple locations are possible, the algorithm shown in chapter 2.3 is applied (*FINDCELL.M*). Notice that such algorithm is implemented as a separate M-file in order to easily allow model improvement as new evidence is provided by biological experiments.

The program will create a cell, modifying all the subspaces that are involved in such process, thanks to *CREATECELL.M* . At this stage we associate to each new cell an age (starting intuitively from zero and upgrading its value as time elapse).

Growth factor redistribution follows the rules explained in section 4.2 and is modeled in *PUSH_GF.M* . The user may set all the parameters for the “pressure wave” that is generated after a new cell is born:

- Radial diffusion
- Multiple waves and GF percentage in each wave

The fractones will be activated/deactivated automatically as the user may define the exact timing (defined by the number of duplications occurred but this assumption can be straightforwardly relaxed setting time as the trigger event, for instance) and position. Whenever during a simulation the user figures out that there is a need to change the displacement of the fractones, this will be done just stopping the simulation and running *RESTART_SIM*. The program will prompt for new fractones' position (several changes may be performed by the user: i.e. GF may be added) and the simulation will be resumed.

5.4 Data plotting

We can choose between two options to plot the results, as shown in pervious simulations:

- 2 dimensional plot, with cells and fractones represented as circles. In this plot GF will not show up (*PLOT_CIRCLES.M*)
- 3 dimensional plot, with cells and fractones as squares and GF as bars (*PLOT_TOGETHER.M*)

We already pointed out that the model may mimic complex cells configurations and with a large number of active fractones it may result difficult to understand which cell undergoes mitosis. For this reason we marked the cells undergoing mitosis (both the "mother" and the "child" cell, but in a different way in order to identify them) and it is possible in both plots to highlight those cells. Finally, all simulations are saved in jpeg image files.

6. APPLICATION TO LAYOUT OPTIMIZATION

The control model developed during this research determines a cellular proliferation process that mimics the developmental stages of natural organisms. These laws can be evolved to respond to desired requirements, and thus be used to search for high-performing engineering layouts. One possibility is to use environment cues for crafting the control laws determining the placement of the fractones. For instance, in a problem to minimize the mass of material to sustain a load, the stress level in the cells may be used as a parameter controlling the creation of a fractone when the stress level on a cell surpass a fixed threshold.

An exploratory result is presented in the following section, where it is shown the cellular division following the inclusion of a fractone on a cell when its level stress exceeded a preassigned limit. A typical solution in structure analysis is to add material nearby those elements where a Von Mises stress higher than a set level is calculated. We will follow this path, activating a fractone next to the cell with the highest stress level in order to relief its condition.

Notice that in this case there is a one to one correspondence between cells and finite elements representing the mechanical structure (i.e. a cantilever beam). The first goal is to reach a compact structure (1-connected, recall section 3.3) that connects the structure to the loads fulfilling prescribed boundary conditions (i.e. supports and constraints).

Notice that the mitosis algorithm has not been changed, but we only activate a fractone associated to the cell with the highest stress level.

6.1 MATLAB code explanation

The first issue that we have to face is to find a code that is able to provide the useful information for fractone placement. We decided to use the program developed by Bendsøe and Sigmund ([41]) in the TopOpt research group[4]. TopOpt's model (called *TOP88.M*) is developed under MATLAB and this allowed us to a quicker implementation into our system.

We merged the two codes then, so that we can start defining the ambient space and the initial configuration of cells in *DEFINE_SPACE.M*, and then in *TOP88.M* we only have to define loads and constraints for the mechanical structure. At this point TopOpt's code creates a stress map of the structure, letting us identify where the fractone has to be placed. The system will count a new cell as soon as the fractone reaches the set threshold (as explained above) and *TOP88.M* will create a new stress map. Iteratively, we will get to the final desired configuration.

In Figure 29 we present a preliminary result where the cell configuration is on the left column and the stress map is on the right, choosing to fill half of the ambient space with cells. Notice that comparing a 3D figure with a two dimensional one, may lead to misinterpretation due to different axis direction but one may check that the results have only different orientation. In order to highlight the last cell undergoing mitosis, we marked its center with a unit in green.
The simulation will start with a configuration of four cells that is not connected, reaching the final desired configuration.

[4] TopOpt is an acronym for Topology Optimization. The TopOpt group is a joined research effort between the departments of Mechanical Engineering and Mathematics at the Technical University of Denmark with the aim of promoting theoretical extensions and practical applications of the topology optimization method.
For further information and to download the source code used for our simulations please visit http://www.topopt.dtu.dk/

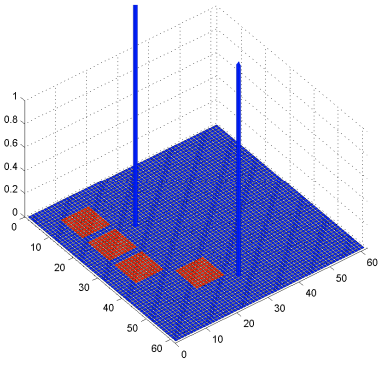
1
0.8
0.6
0.4
0.2
0
0
10
20
30
40
50
60
0
10
20
30
40
50
60

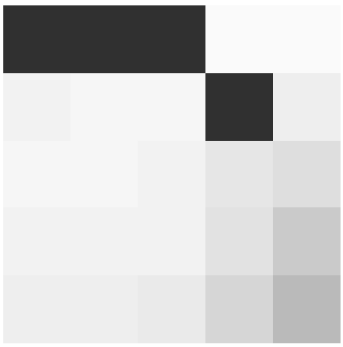

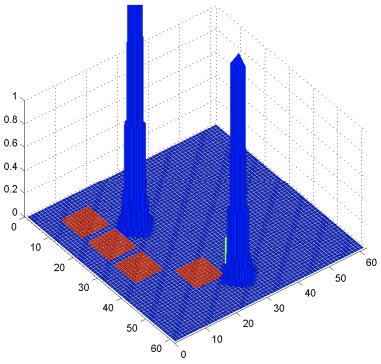
1
0.8
0.6
0.4
0.2
0
0
10
20
30
40
50
60
0
10
20
30
40
50
60

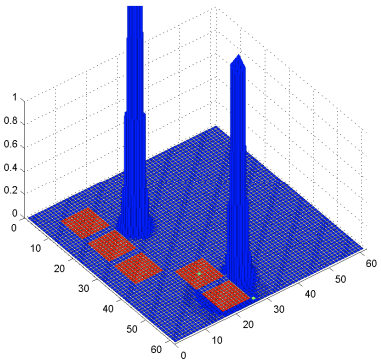
1
0.8
0.6
0.4
0.2
0
0
10
20
30
40
50
60
0
10
20
30
40
50
60

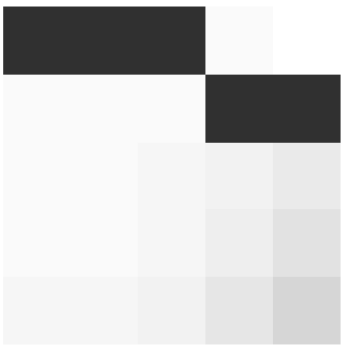

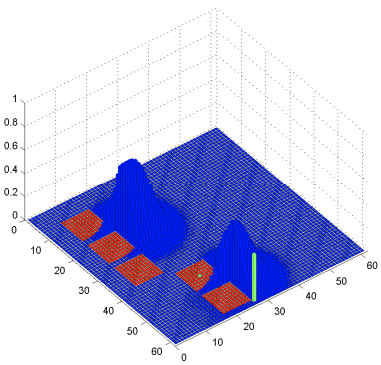
1
0.8
0.6
0.4
0.2
0
0
10
20
30
40
50
60
0
10
20
30
40
50
60

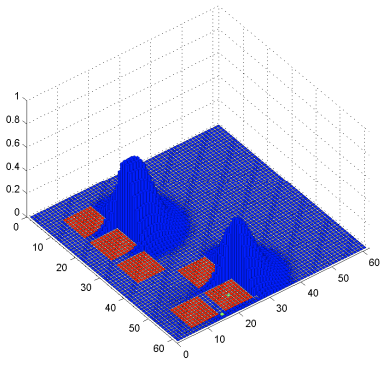
1
0.8
0.6
0.4
0.2
0
0
10
20
30
40
50
60
0
10
20
30
40
50
60

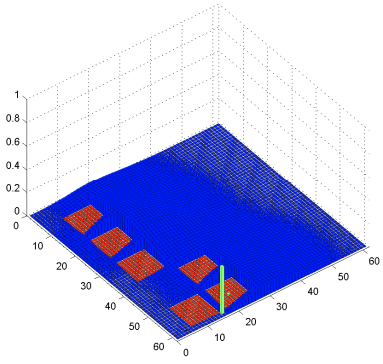
1
0.8
0.6
0.4
0.2
0
0
10
20
30
40
50
60
0
10
20
30
40
50
60

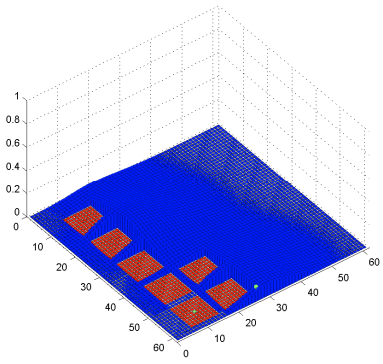
1
0.8
0.6
0.4
0.2
0
0
10
20
30
40
50
60
0
10
20
30
40
50
60

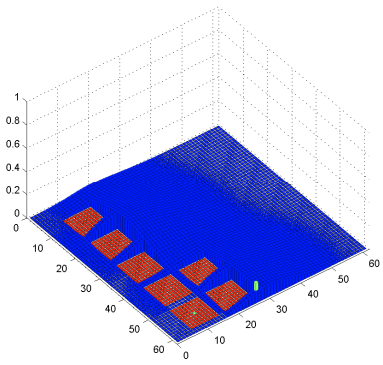
1
0.8
0.6
0.4
0.2
0
0
10
20
30
40
50
60
0
10
20
30
40
50
60

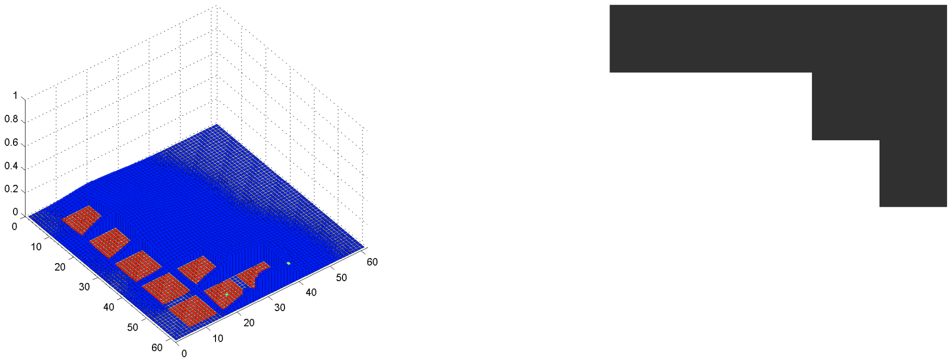

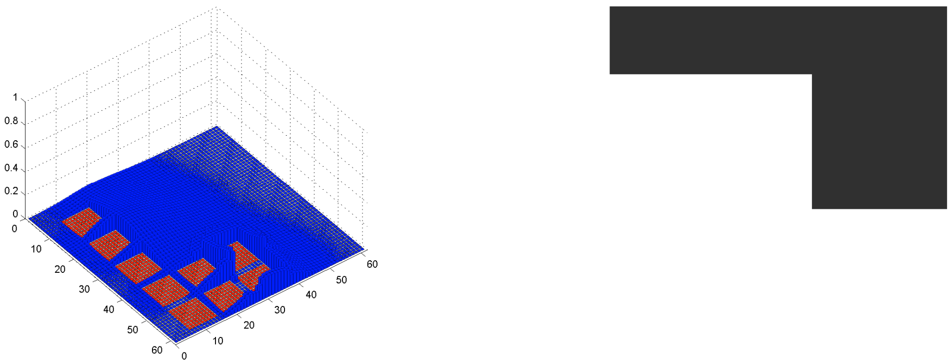

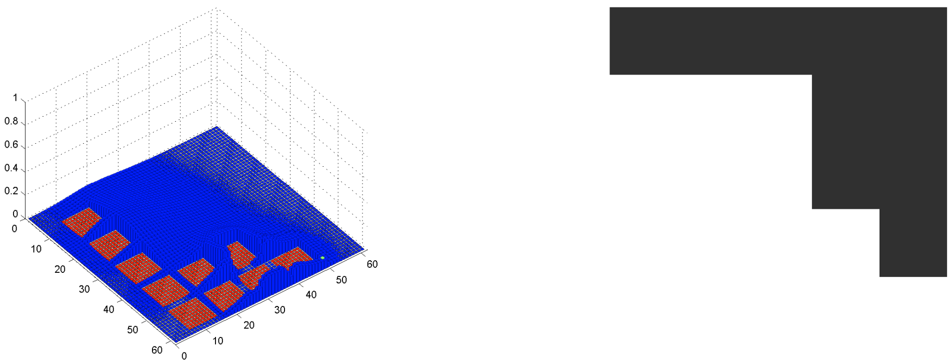

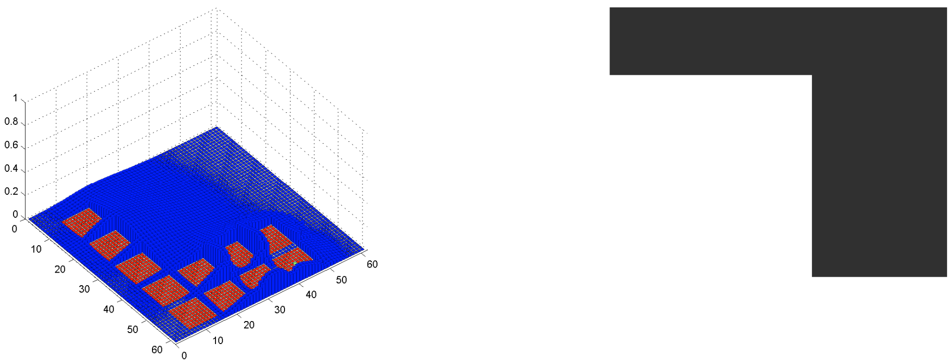

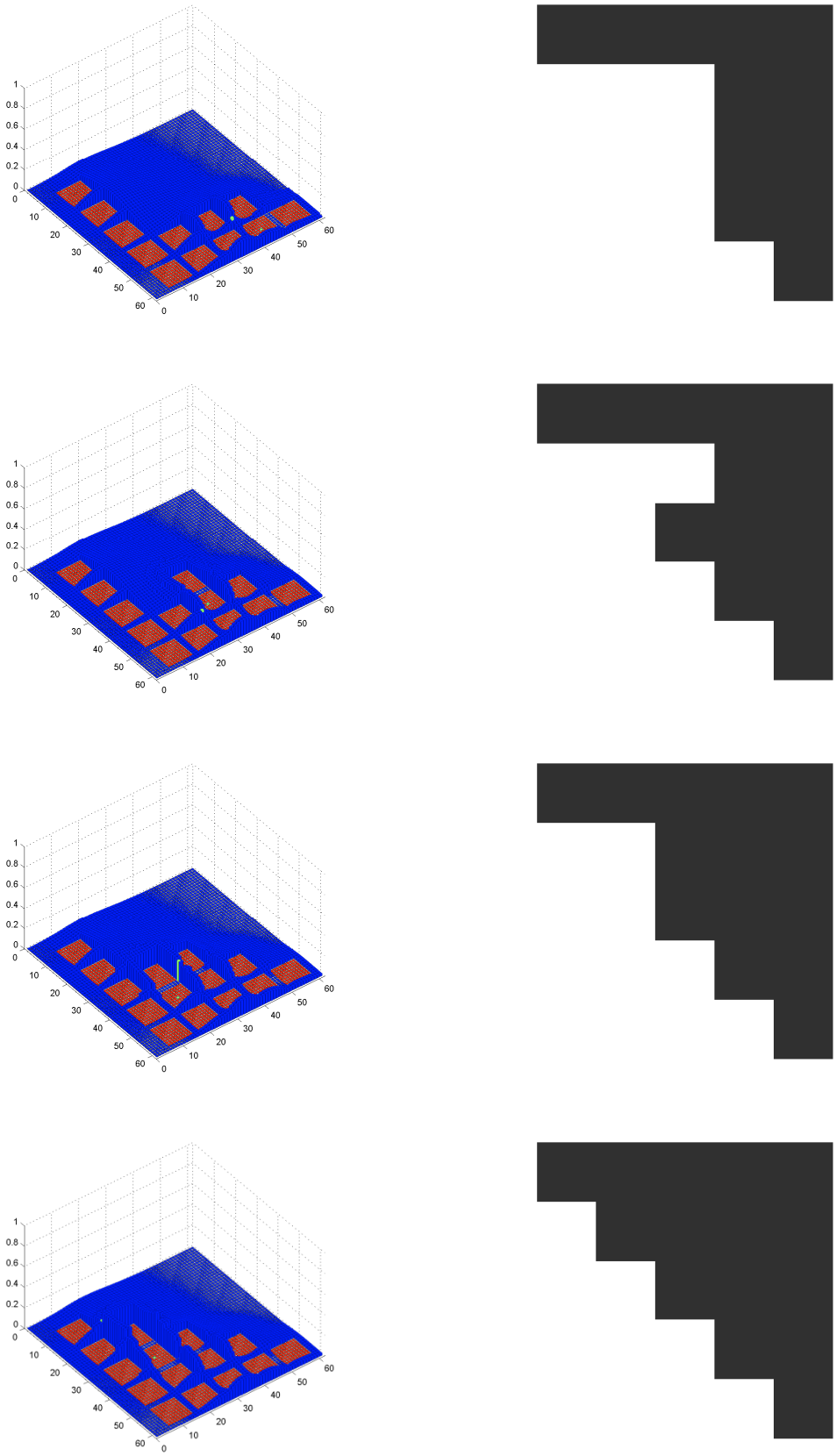

Figure 29 - Application to layout optimization

The model may be straightforwardly upgraded allowing cell death, that is removing additional material from a mechanical structure because it is not necessary for structural purposes. This can be done setting a minimal stress value, under the one a cell will be removed. Another improvement that would lead to a faster convergence to the desired solution is to modify the mitosis algorithm, giving birth to directional mitosis (recall that now new cells are placed in an arbitrary clockwise direction) based on stress maps. It is clear that this process would bring us far from the biological statement and for this reason is not treated in this study.

The result of the application of a simplified version of the procedure without the diffusion of the growth factor is shown in Figure 30 - note that in this form the method is similar to bi-directional evolutionary structural optimization methods (see e.g. [46]).

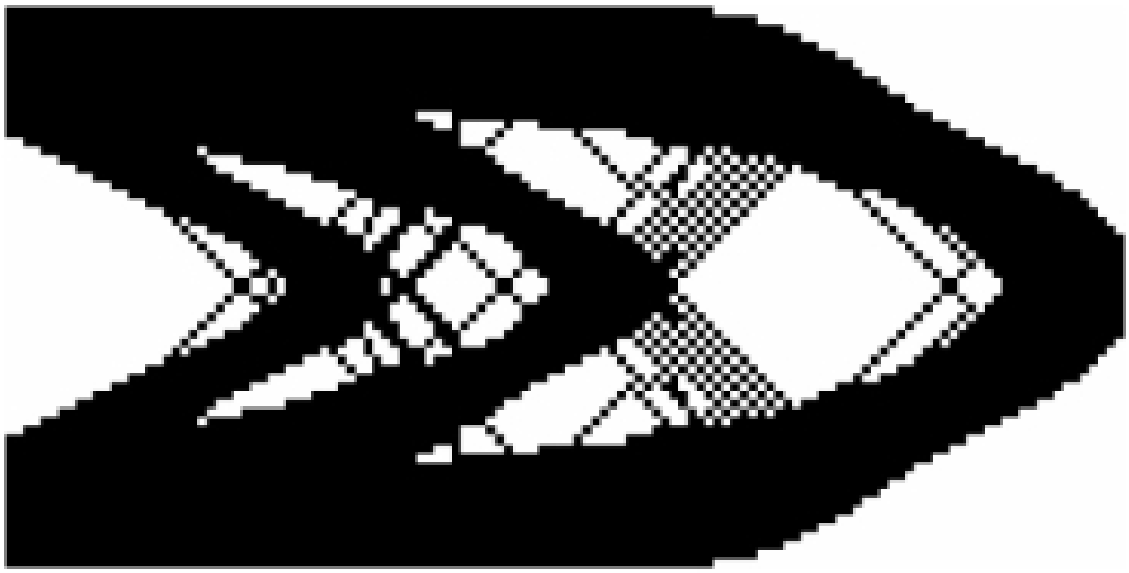

Figure 30 - Preliminary result for layout optimization of a cantilever

7. FUTURE WORK

Inspired by biological discoveries, we proposed to develop and analyze a mathematical model predicting cell proliferation from the spatial distribution of fractones. Our primary goal is to develop a model that contains the crucial features of our hypothesis and, at the same time, is sufficiently simple to allow an understanding of the underlying principles of the observed system.

There are mainly two directions of work that we are planning to undertake at this stage. First, from a purely mathematical perspective, an open question is the development of new techniques to answer controllability and optimality questions for control systems such as the one introduced in this paper. Second, the interplay between the biological motivation and the mathematics must be refined to predict neurulation and post-neurulation growth by the mathematical model using fractone maps produced by biological research.

The current model is based on what we believe are the most critical features of our hypothesis. However, some of our assumptions are very restrictive and we also need to add some complexity to produce a more realistic model. Other important features of the biological system that have not yet been taken into account will be incorporated into our model. However, despite the new features to be added, the statement of the problem will generally remain the same.

After all of this has been accomplished, we will discretize the fractone maps provided by biologists and then determine whether the prediction of the mathematical model reflects the growth of the neural tissue observed in the maps. The observation of spatial distribution of fractones provided by the maps will determine the control function to be used in the mathematical model to produce our simulations.

Our future work will take into account the diffusion of different type of growth factor and different sensitivity of fractones to growth factors. This extension is straightforward

and has not been introduced into our model in order to avoid adding unnecessary complexity to our model, preserving all the efforts for crucial topics.

The proposed model will be developed by having cells that are not vertically and horizontally aligned and a three dimensional model. These two steps will need new rules to be defined (i.e. in the three dimensional case, how would the different layers interact? How will this affect the mitosis algorithm?) driven by new observations from the experimental maps.

8. CONCLUSIONS

Through this work, we made a first step in a complex field, creating a code that mimics the biological system behavior, to help us to understand the nonlinear dynamics of the system under study. Our model clearly diverges from Turing's model (or any other Reaction-Diffusion model), and it presents new challenges that will advance the field of control theory. To envision how our model does this, we must compare and contrast versus typical control theory problems. For example, in physics, the state space is static and the equations of motion are derived from minimizing a Lagrangian. In engineering, the configuration manifold is fixed and one either attempts to determine the evolution of the system while minimizing a prescribed cost or one tries to design controls to take into account uncertainties of the system. Due to the morphogenic nature of the biological process under study, the configuration space is constantly evolving (caused by the creation of new cells), and thus the control model we developed cannot be analyzed using traditional techniques of control theory in which the equations describing a given system are predetermined when defining the system. This distinguishes in a very non-trivial way our problem from the traditional problems whose systems are usually defined on a static configuration space.

The current model is based on what we believe are the most critical features of our hypothesis. However, some of our assumptions are very restrictive and will be relaxed as new evidence is provided by experimental results; to easily accomplish this goal we produced a versatile and flexible code, as shown by the example in Figure 29.

The research has been pursued keeping always in mind that modeling such a broad biological system may lead to unacceptable arbitrariness. In order to avoid it, we tried to keep the model as simple as possible.

Finally, we would remark that the aim of this study is not to create a model that mimics exactly the biological process under study, rather than creating a good model that may be developed in future thank to new experimental results and propose new questions that may bring to an advance in the field of control theory. This a complex

field and new rules have to be defined, as this problem cannot be solved and analyzed through classic control theory techniques. We will have to propose innovative ideas and methods to analyze and to answer controllability and optimality questions.

Several publications arise from this study: see [47], [48], [49] as a preliminary list.

REFERENCES

1 Kerever A, Schnack J, Vellinga D, Ichikawa N, Moon C, Arikawa-Hirasawa E, Efird JT, Mercier F. Novel extracellular matrix structures in the neural stem cell niche capture the neurogenic factor fibroblast growth factor to from the extracellular milieu. *Stem Cells 25* (2007), 2146-2157.

2 Mercier F, Kitasako JT, Hatton GI. Anatomy of the brain neurogenic zones revisited: fractones and the fibroblast/macrophage network. *J Comp Neurol 451* (2002), 170-188.

3 Mercier F, Kitasako JT, and Hatton GI. Fractones and other basal laminae in the hypothalamus. *J Comp Neurol 455* (2003), 324-340.

4 M, Hannon B and Ruth. *Modeling Dynamic Biological Systems*. Springer-Verlag, Series: Modeling Dynamic Systems, New York, 1997.

5 M, Chyba. Autonomous Underwater vehicles Ocean Engineering. *Special Issue on Autonomous Underwater Vehicles*, 36/1, 1-132.

6 Chyba M, Haberkorn T, Smith, RN, and Choi, SK. Autonomous Underwater Vehicles: Development and Implementation of time and Energy Efficient Trajectories. *Ship Technology Research,* 55/2 (2008), 36-48.

7 M, Piccoli B and Garavello. Traffic Flow on Network. *AMS book series, Applied Math Series. n.1, American Institute of Mathematical Sciences* (2006).

8 ED, Sontag. Some new directions in control theory inspired by systems biology. *IET Systems Biology* (2004), 9-18.

9 ED, Sontag. Molecular systems biology and control. *Eur. J. Control*, 11(4-5) (2005), 396-435.

10 N., Wiener. *The Extrapolation, Interpolation and Smoothing of Stationary Time Series*. John Wiley and Sons, Inc., New York, 1949.

11 WB, Cannon. *The wisdom of the body*. Norton, New York, 1932.

12 RE, Kalman. On the General Theory of Control Systems. (Moscow, USSR 1960), Proceedings First International Conference on Automatic Control.

13 von Bertalanffy, L. *General System theory: Foundations, Development, Applications*. George Braziller, 1968.

14 Hodgkin AL, Huxley AF. A quantitative description of membrane current and its application to conduction and excitation in nerve. *J Physiol* (1952).

15 D, Noble. A modification of the Hodgkin-Huxley equations applicable to Purkinje fibre action and pacemaker potentials. *J Physiol* (1962).

16 Mesarovic, MD. *Systems Theory and Biology*. 1968.

17 D, Bernoulli. *Essai d'une nouvelle analyse de la mortalité causée par la petite vérole, et des avantages de l'inoculation pur la prévenir*. Histoire de l´Acad. Roy. Sci. avec Mém. des Math. et Phys. Mém., Paris, 1760.

18 L, Euler. *Recherches générales sur la mortalité et la multiplication.* Mémoires de l'Académie Royal des Sciences et Belles Lettres, 1760.

19 Euler, L. *Principia pro moto sanguinis per arterias determinando*. 1775.

20 PF, Verhulst. *Notice sur la loi que la population suit dans son accroissement*. Correspondance mathématique et physique publiée par A. Quételet, Brussels, 1838.

21 F, Galton. *Natural inheritance*. Macmillan, London, 1889.

22 Pearson K, Lee A. *On the laws of inheritance in man*. Biometrika 2, 1903.

23 AA, Markov. *Extension of the law of large numbers to dependent variables [Russian]*. Izv Fiz-Matem Obsch Kazan Univ, 1906.

24 GH, Hardy. *Mendelian proportions in a mixed population*. Science 28, 1908.

25 AJ, Lotka. *Elements of physical biology*. Williams and Wilkins, Baltimore, 1925.

26 V, Volterra. Variations and fluctuations of the number of individuals in animal species living together. In RN, Chapman, ed., *Animal ecology*. McGraw Hill, New York, 1931.

27 Kolmogorov A, Petrovsky I, Piscounov N. *Etude de l'équation de la diffusion avec croissance de la quantité de matière et son application à un problème biologique*. Moscow University, 1937.

28 Luria SE, Delbrück M. Mutations of bacteria from virus sensitivity to virus resistance. *Genetics* (1943).

29 DG, Kendall. Stochastic processes and population growth. *J R Stat Soc* (1949), 230-264.

30 AM, Turing. The chemical basis of morphogenesis. *Phil Trans R Soc Lond B Biol Sci*, 237 (1952), 37-72.

31 von Neumann J, Morgenstern O. *Theory of games and economic behavior*. John Wiley and Sons, New York, 1953.

32 S, Benzer. On the topology of the genetic fine structure. (1959), Proc Natl Acad Sci USA.

33 Erdös P, Rényi A. On the evolution of random graphs. *Publ Math Inst Hung Acad Sci* (1960), 17-61.

34 WJ, Ewens. The sampling theory of selectively neutral alleles. *Theor Popul Biol* (1972), 87-112.

35 JFC, Kingman. On the genealogy of large populations. *J Appl Prob* (1982), 27-43.

36 M, Kimura. *Population genetics, molecular evolution, and the neutral theory*. University of Chicago Press, Chicago, 1994.

37 MA, Savageau. *Biochemical systems analysis: a study of function and design in molecular biology*. AddisonWesley, Reading, MA, 1976.

38 J, Higgins. Analysis of sequential reactions. *Ann. New York Acad. Sci.*, 108 (1963), 305-321.

39 DE, Koshland. Application of a Theory of Enzyme Specificity to Protein Synthesis. *Proc. Natl. Acad. Sci. U.S.A.* , 44 (2) (1958).

40 WR, Ashby. *An Introduction to Cybernetics*. Chapman and Hall, London, 1956.

41 M. P. Bendsøe, O. Sigmund. *Topology Optimization: Theory, Methods and Applications*. Springer, New York, 2003.

42 H. A. Eschenauer, N. Olhoff. Topology optimization of continuum structures: A review. *Applied Mechanics Reviews*, 54.

43 Rozvany, G. I. N. Aims, scope, methods, history and unified terminology of computer-aided topology optimization in structural mechanics. *Structural and Multidisciplinary Optimization*, 21.

44 Bourdin, B. Filters in topology optimization. *International Journal for Numerical Methods in Engineering*, 50 (2001), 2143-2158.

45 C. Ronse, M. Tajine. Discretization in Hausdorff space. *Journal of Mathematical Imaging and Vision*, 12, 3 (2000), 219-242.

46 Querin, O. M., Young, V., Steven, G. P., and Xie, Y. M. Computational efficiency and validation of bi-directional evolutionary structural optimization. *Computer methods in applied mechanics and engineering*, Vol. 189, 2 (2000).

47 M. Chyba, J. Marriott, F. Mercier, J. Rader, G. Telleschi.. Modeling Cell Fractone Dynamics Using Mathematical Control Theory. (Florida - U.S.A. 2011), 50th IEEE Conf. on Decision and Control.

48 M. Chyba, F. Mercier, J. Rader, A. Tamura-Sato, Y. Kwon, G. Telleschi. Using Control Theory To Model Neural Morphogenesis. *Journal of Math-for-Industry, Japan.*

49 M. Chyba, M. Kobayashi, F. Mercier, J. Rader, A. Tamura-Sato, G.

Telleschi, Y. Kwon. A new Approach to Modeling Morphogenesis Using Control Theory. *Special volume of the São Paulo Journal of Mathematical Sciences in honor of Prof. Waldyr Oliva* (To Appear 2012).